A New Appraisal of Sri LankanBB Zircon asReference Material for LA-ICP-MS U-Pb Geochronology and Lu-Hf Isotope Tracing

Maristella M. **Santos**(1, 2)*, Cristiano **Lana**(1), Ricardo **Scholz** (1), Ian **Buick** (3), Mark D. **Schmitz** (4) , Sandra L. **Kamo** (5), Axel **Gerdes** (6), Fernando **Corfu** (7),Simon **Tapster** (8), Penelope **Lancaster** (9), Craig D. **Storey** (9), Miguel A.S. **Basei** (10),Eric **Tohver** (11) , Ana **Alkmim** (1), Herminio **Nalini**(1), Klaus **Krambrock** (12), Cristiano **Fantini** (12), Michael **Wiedenbeck** (13)

(1)Applied Isotope Research Group, Departamento de Geologia, Escola de Minas, Universidade Federal de Ouro Preto, Campus Universitário Morro do Cruzeiro s/n, 35400-000 Ouro Preto – MG, Brasil.
(2) Instituto Federal de Minas Gerais (IFMG), Campus Congonhas, Minas Gerais, 36415000, Brazil
(3) Centre for Crustal Petrology, Dept. of Earth Sciences, Stellenbosch University, Private Bag X1, Matieland 7602, Stellenbosch, South Africa
(4) Department of Geosciences, Boise State University, 1910 University Dr., Boise, ID 83725, USA
(5) Jack Satterly Geochronology Laboratory, Department of Earth Sciences, University of Toronto, 22 Russell St., Toronto, Ontario, M5S 3B1, Canada
(6)Institute of Geosciences, Johann Wolfgang Goethe University, Altenhöferallee 1, D-60438 Frankfurt am Main, Germany
(7)Department of Geosciences, University of Oslo, Postbox 1047 Blindern, N-0316 Oslo, Norway
(8) NERC Isotope Geosciences Laboratory, British Geological Survey, Kingsley Dunham Centre, Keyworth, Nottingham NG12 5GG, UK
(9)School of Earth and Environmental Sciences, Burnaby Building, University of Portsmouth, Portsmouth, PO1 3QL, UK
(10)Centro de Pesquisas Geocronológicas – CPGeo/IGc – USP, São Paulo, SP, Brazil
(11)Tectonics Special Research Center, University of Western Australia, Perth, WA, Australia
(12) Departamento de Física, Universidade Federal de Minas Gerais, 31.270-901 Belo Horizonte, MG, Brazil
(13)Deutsches GeoForschungZentrum, Telegrafenberg, 14473 Potsdam, Germany
* Corresponding author. e-mail: maristella.santos@hotmail.com

Abstract: A potential zircon reference material (BB zircon) for Laser Ablation-Inductively Coupled Plasma-Mass Spectrometry (LA-ICP-MS) U-Pb geochronology and Hf isotope geochemistry is described. A batch of zircon megacrysts (0.5 to 1.5 cm^3) from Sri Lanka were investigated. Within-grain rare earth element(REE) compositions are largely homogeneous, albeit with some variation seen between fractured and homogeneous domains. Excluding fractured cathodoluminescence bright domains, the variation of U content for all analyzed crystals ranges from 227 to 368 μg g^{-1} and the average Th/U ratios span between 0.20 and 0.47. The Hf isotopic composition (0.56 - 0.84 g/100g Hf) is homogenous within and between the grains - mean $^{176}Hf/^{177}Hf$ of 0.281674 ± 0.000018 (2SD). The calculated alpha dose of 0.59×10^{18} g^{-1} is within the trend of previously studied, untreated zircon samples from Sri Lanka. Aliquots of the same crystal (given to four different ID-TIMS laboratories) gave consistent results with excellent measurement reproducibility (0.1-0.4% RSD). Interlaboratory assessment (via LA-ICP-MS) from twenty individual crystals returned results that are within uncertainty equivalent to the TIMS ages. Finally, we report on within and between grain homogeneity of the oxygen isotopic systematic of four BB crystals (13.16‰VSMOW).

Keywords: BB zircon, Sri Lankan reference material, U-Pb geochronology, Hf isotopic system, Rare Earth Elements, LA-ICP-MS

Introduction

Zircon, of the available accessory phases used for U-Pb geochronology, has the greatest utility because of its occurrence in a wide range of sedimentary, igneous and metamorphic rock types, its great resistance to weathering, its low initial common Pb up-take and low Pb diffusivity (e.g., Speer 1982,Cherniak and Watson 2003). Hafnium substitution into the zircon lattice up to g/100gmass fractions (rarely less than 0.3-0.5 g/100g of Hf) makes it effective for tracking crustal evolution in magmatic rocks and fingerprinting detrital zircon populations through its composition. Additionally, the oxygen isotope composition in zircon is robust even through metamorphism and can be used as a petrogenetic tracer (e.g., Valley 2003). The low diffusivity of elements within the zircon lattice (Cherniak and Watson 2003) means that individual zircon crystals commonly preserve multiple compositional and (U-Th-Pb, Hf and O) isotopic domains, even after having experienced magmatic and/or high temperature metamorphic cycles. Analysis of intercrystal domains require high-spatial resolution analytical approaches such as SIMS (Secondary Ionisation Mass Spectrometry) or LA-ICP-MS (Laser Ablation-Inductively Coupled Plasma-Mass Spectrometry) to unravel complex zircon growth histories.

The increasingly widespread use of instruments capable of high-spatial resolution isotopic analysis through destructive methods is driving the development of new matrix-matched reference materials for U-Pb geochronology and isotope geochemistry in general. Zircon has also been used, with variable degrees of success, as the calibrant for non-matrix-matched dating of other accessory phases, for which U-Pb reference materials are difficult to obtain, or do not exist (e.g., xenotime, cassiterite, columbite-tantalite, scheelite, perovskite; Gulson and Jones 1992, Batumike *et al.* 2008, Dewaele *et al.* 2011, ZhiChao *et al.* 2011). Natural zircons must be used because of the difficulty of inserting Pb into synthetic crystals (e.g. Wiedenbeck *et al*. 1995, Black *et al.* 2003, Jackson *et al.* 2004, Nasdala *et al.*

2008, Sláma *et al.* 2008). It is important to realize that some level of natural variation is expected and observed within all reference materials and the level of characterization is in part a function of the number/scale of characterization experiments, which in the case of this work is exceptionally large and employs multiple independent laboratory techniques.

There are a number of natural zircons used as reference materials for geochronology and isotope geochemistry, including 91500 (megacrysts probably from syenitic pegmatite; Wiedenbeck *et al*. 1995), Mud Tank(megacrysts from carbonatite; e.g., Woodhead and Hergt 2005), GJ-1(; Jackson *et al.* 2004), M257 (Sri Lankan magacryst; Nasdala *et al.* 2008), Temora (~200 by 100 micron zircons sourced from monzodiorite; Black *et al.* 2003) and Plešovice (megacrysts from an alkaline granulite; Sláma *et al.* 2008). This study presents isotopic data for a natural zircon material that appears to be a suitable reference material for U-Pb dating and Hf isotopic measurements by LA-ICP-MS. Our analyses focused on the determination of reliable values of U-Pb age, Hf-isotopic ratios, REE, U and Hf mass fractions.

Geological background and sample description

The zircon samples for this study come from a placer deposit of the Ratnapura gemstone field (Dissanayake and Rupasinghe 1993), located in the southwestern region of the Sri Lankan Highland Complex (Kröner *et al.*1994b). The Highland Complex is composed of mafic and quartzofeldspathic granulites, charnockitic rocks, marble and quartzite, all metamorphosed tohigh- and ultrahigh-temperature granulite-facies conditions (Kröner *et al.* 1994b, Dissanayake *et al.* 2000,Sajeev *et al.* 2010). Extensive U-Pb isotopic studies, including the application of high-spatial resolution techniques such as sensitive high mass resolution ion microprobe (SHRIMP) analysis, have contributed towards establishing a geochronological framework for the high-grade rocks of Sri Lanka(e.g., Hölzl *et al.* 1994, Kröner *et al.* 1994a, Nasdala *et al.* 2004, Sajeev *et al.* 2010, Santosh *et al.* 2014, Dharmapriya *et al.* 2015). In

particular, geochronologic data have shown that the Highland Complex experienced a prolonged/polyphase granulite-facies history from *ca*. 580 to 530 Ma.

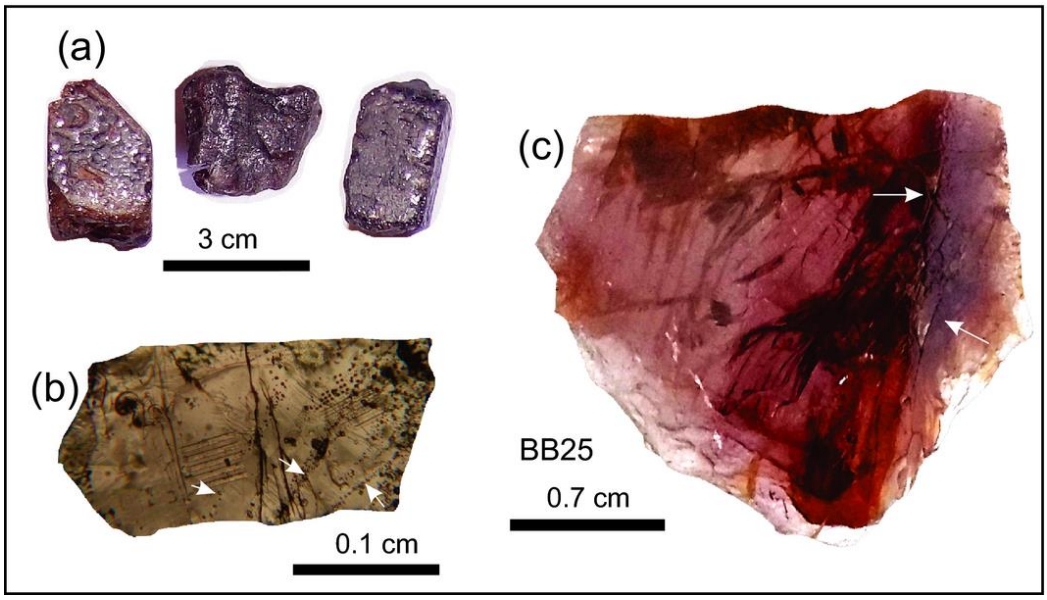

Figure 1: (a) BB zircons with colour and subhedral shapes. (b) Transmitted light image of a small fragment of BB17 showing fracture zones, a small pit and inclusions (white arrows). (c) Whole-grain imaging via transmitted light of BB25 showing fractured domain (white arrows).

*Circa*300 g of zircon megacrysts, comprising some eighty grains and hereafter referred as to as Blueberry (BB) zircons, were acquired and numbered for the present study. We have selected 20 individual crystals (comprising 110 g) of this lot that are dark purple in color, translucent and commonly larger than 10 mm (Figure 1a, c). The largest (>10mm-wide) megacrysts (BB9, BB12 and BB17) were broken into hundreds of small (1-2 mm wide) inclusion-free fragments that show only weak oscillatory zoning in cathodoluminescence (CL) images (Figure 2a). A small sub-set of these BB fragments are, however, marked by fractured domains (e,g. Figure 1b, c) and patchy CL zoning (Figure 2b, c). These domains are commonly associated with inclusions and small (>10 μm) internal dissolution pits. Five other megacrysts (BB2, BB11, BB13, BB25 and BB39) were sectioned by polishing to reveal internal features (e.g., Figures 1c and 2b). Most parts of such megacrysts are homogeneous, or show only weak CL zoning, or show small domains or rims that are rather bright under CL imaging (e.g.

Figure2b).Other megacrysts such as BB25 showed large domains with a number of fractures, pits and minor mineral inclusions (Figure2b). Fractures are common around the rims and are often filled with recrystallized zircon (Figure2c). These domains were excluded from further characterization.

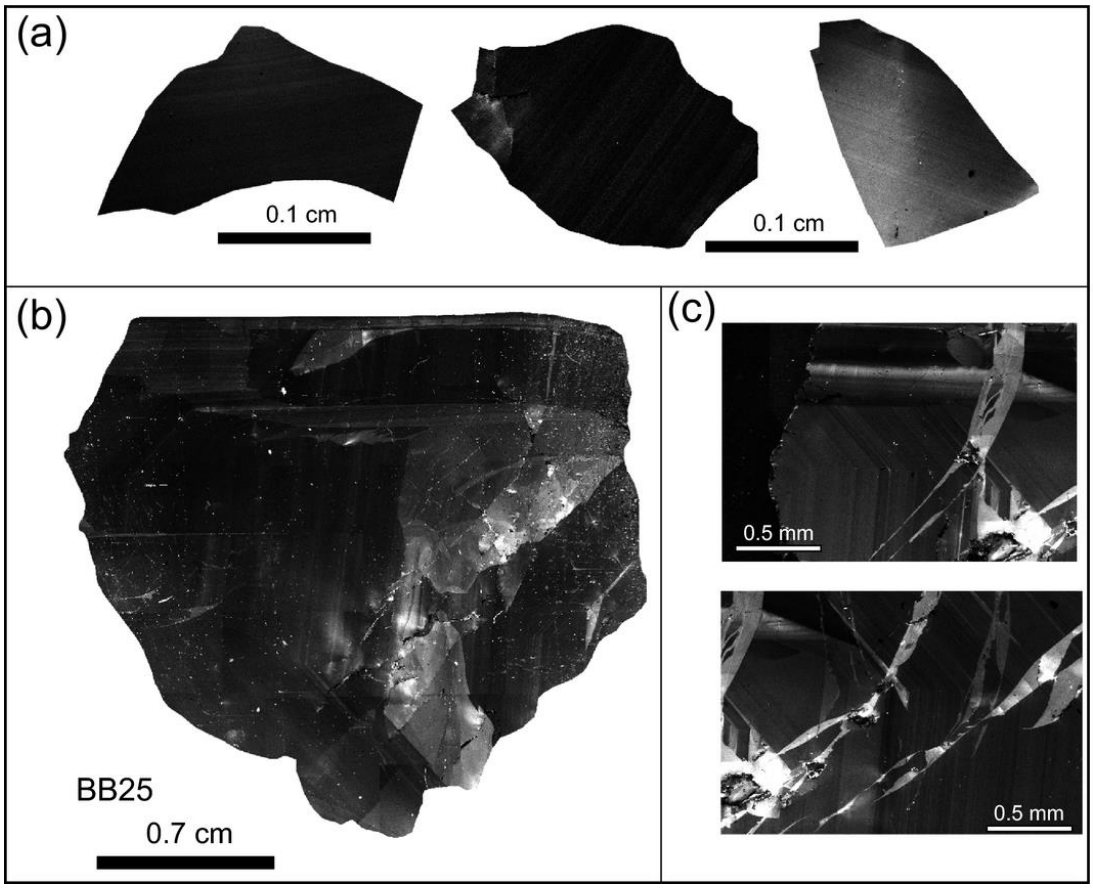

Figure 2: (a) Cathodoluminescence (CL) images of fragments of BB megacrysts (grains BB9, BB12 and BB17), showing rather homogeneous domains marked by thin/weak oscillatory zoning. (b) Whole-grain CL imaging of BB25 showing homogeneous, low CL domains and bright, fractured domains. For comparison, note that light cathodoluminescence correlates with a high density of fractures (right portion of BB25) shown in Figure 1b. (c) Detailed CL image of fractured domains of BB12 – note that fractures have been sealed with recrystallised zircon.

Analytical methods

Previous studies have established key requirements for minerals such as zircon to be considered as reference material for U-Pb and Hf isotopes analyses by LA-ICP-MS (e.g., Wiedenbeck *et al.* 1995, 2004, Black *et al.* 2003, Jackson *et al.* 2004, Sláma *et al.* 2008, Li*et al.*2010, Gonçalves *et al.* 2016). First, the mineral must be dated with high precision and accuracy by independent methods, there must be limited variability in both U-Pb age and Hf isotopic compositions. Furthermore, moderate U (tens to hundreds μg g^{-1}) and adequate Hf (a few percent) contents, low common Pb as well as low Lu/Hf and Yb/Hf ratios are desirable. With respect to oxygen isotopic characteristics, demonstrable homogeneity at the nanogram sampling level at uncertainty levels better than offered by micro analytical methods (i.e., ± 0.2 ‰ (2SD) or better). The material should be sufficiently large for repeated analyses by laser ablation (grains several millimeters to centimeters in diameter) and should be available in large quantities for distribution to the scientific community and for enabling data traceability between analytical facilities.

To ensure extensive characterization of the zircon investigated in this study, chemical and isotopic analyses were conducted using a number of different techniques (Table 1) in several laboratories: ***ID-TIMS*****:** Jack Satterly Geochronology Laboratory (JSGL; Canada), NERC Isotope Geosciences Laboratory (NIGL; UK), University of Oslo (Norway), Boise State University (BSU; USA); ***U-Pb LA-ICP-MS*****:** J.W. Goethe University of Frankfurt am Main (JWG; Germany), Federal University of Ouro Preto (UFOP; Brazil), University of Portsmouth(UK), University of São Paulo (USP; Brazil); ***Trace Element LA-ICP-MS*****:** Federal University of Ouro Preto (UFOP; Brazil); Lu-Hf isotope ***LA-ICP-MS*****:** J.W. Goethe University of Frankfurt am Main (JWG; Germany), Federal University of Ouro Preto (UFOP; Brazil); ***Cathodoluminescence imaging*****: UFOP**; ***Raman spectroscopy*****:** Federal University of Minas Gerais (UFMG; Brazil); ***X-ray powder diffraction*****:** UFOP. Where possible, the measurements

were reproduced by similar techniques in different laboratories. See Table 1 for a full summary of the methods employed on the 20 BB crystals.

For the characterization of the U-Th-Pb systematics, we selected fragments of the BB crystals and these were distributed to various TIMS and LA-ICP-MS laboratories. Some of the largest fragments were distributed only to LA-ICP-MS laboratories (Table 1). The key objective here was to perform a blind test to assess age variations between and within individual grains. For details on the methodology and instrumentation, see Appendix A. For trace element characterization, synthetic silicate glass NIST-612 was used as the calibrating reference and stoichiometric Si (SiO2 = 32.78 wt%) was used as the internal standard.

With respect to our investigation of the isotopic systematics of the BB sample suite, a mount was prepared that contained 2 or 3 fragments from each of the crystals BB9, BB12, BB25 and BB39. Furthermore, the same epoxy mount included the zircon reference materials 91500, Temora2 (Black *et al*. 2004), Plešovice and Penglai (Li *et al*. 2010) (Appendix B). We used the Cameca 1280-HR SIMS instrument in Potsdam (Deutsches GeoForschungZentrum; GFZ) to conduct a total of 227 $^{18}O^{-}/^{16}O^{-}$ determinations during a 17 hour period run in fully automated mode. The SIMS instrumental set-up followed that of Nasdala *et al*. (2016), with the modification that spots were not run in duplicate. Calibration of the instrument was based on the 91500 zircon, which has a $\delta^{18}O$ SMOW (Standard Mean Ocean Water) calibrated value of 9.86 ± 0.11 as based on data from seven gas source mass spectrometry laboratories (Wiedenbeck *et al*. 2004). The total sampling mass for the SIMS oxygen analyses was *circa* 160 pg as based on white light profilometry.

Table 1: Summary of the methods employed on twenty BB zircon crystals

Sample	Number of analyses												
	Trace element composition (LA-SF-ICP-MS) – UFOP	ID-TIMS U-Pb dating				LA-Q-ICP-MS U-Pb dating		LA-SF-ICP-MS U-Pb dating		LA-MC-ICP-MS U-Pb dating		LA-MC-ICP-MS Hf isotope analyses		SIMS isotope analy
		JSGL	NIGL	Oslo	BSU	UFOP	Portsmouth	UFOP	JWG	UFOP	USP	UFOP	JWG	GFZ
BB1	10	–	–	–	–	–	–	–	8	–	–	–	7	–
BB2	10	–	–	–	–	–	–	–	5	–	–	–	13	–
BB3	10	–	–	–	–	–	–	–	14	–	–	–	20	–
BB4	10	–	–	–	–	–	–	–	6	–	–	–	5	–
BB5	10	–	–	–	–	–	–	–	11	–	–	–	16	–
BB6	10	–	–	–	–	–	–	–	10	–	–	–	5	–
BB7	–	–	–	–	–	–	–	–	–	–	–	–	7	–
BB8	10	–	–	–	–	–	–	–	5	–	–	–	–	–
BB9	10	3	8	3	12	12	30	33	21	9	39	17	3	31
BB10	–	–	–	–	–	–	–	18	–	–	–	13	–	–
BB11	–	–	–	–	–	11	–	20	–	–	–	12	–	–
BB12	16	3	–	3	5	15	–	24	–	24	35	15	–	29
BB13	–	–	–	–	–	14	–	19	–	–	–	12	–	–
BB14	–	–	–	–	–	14	–	20	–	–	–	9	–	–
BB16	–	–	–	–	–	13	–	35	29	–	–	16	–	–
BB17	17	–	–	5	5	13	–	24	–	–	38	11	–	–
BB18	–	–	–	–	–	–	–	–	–	–	–	16	–	–
BB25	35	–	–	–	–	–	–	–	–	–	–	–	–	19
BB39	–	–	–	–	–	–	–	–	–	60	–	–	–	30
BBF	–	–	–	–	–	–	–	–	5	–	–	–	–	–

JSGL - Jack Satterly Geochronology Laboratory (Canada), NIGL - NERC Isotope Geosciences Laboratory (UK), Oslo - University of Oslo (Norway), BSU - Boise State University (USA), UFOP - Federal University of Ouro Preto (Brazil), Portsmouth - University of Portsmouth (UK), JWG - J.W. Goethe University (Frankfurt am Main, Germany), USP - University of Sao Paulo (Brazil), GFZ - Deutsches GeoForschungsZentrum (Potsdam, Germany).

Results

Structural study by X-ray powder diffraction and Raman spectroscopy

In order to evaluate the crystallinity of the samples, unit cell parameters were obtained by X-ray powder diffraction (Table 2): $a_0$has a variation between 6.6072 ± 0.0005 Å and 6.6185 ± 0.0004 Å, while c_0 varies between 5.9897 ± 0.0006 Å and 6.0100 ± 0.0005 Å, which results in a unit cell volume rangingbetween261.481 ± 0.080 $Å^3$ and263.265 ±0.090 $Å^3$.As it can be observed in Figure 3, the XRD patterns are marked by well-defined peaks and low background values. The self-irradiation as quantified from the U and Th mass fractions and the zircon age by calculating the time-integrated alpha dose (D_α) according to the formula (Murakami*et al.* 1991, Nasdala *et al.* 2001):

$$D_\alpha = \frac{6.c_{Th}.N_A}{10^6.M_{232}}.\left(e^{\lambda_{232}t}-1\right)+\frac{7.c_U.0.0072.N_A}{10^6.M_{235}}.\left(e^{\lambda_{235}t}-1\right)+$$

$$\frac{8.c_U.0.9928.N_A}{10^6.M_{238}}.\left(e^{\lambda_{238}t}-1\right)$$

where $c_U$and $c_{Th}$are the present actinide mass fractions (in μg g^{-1}), N_A is Avogadro's number, M_{238}, M_{235}, and M_{232} are the atomic weights of the parentisotopes, λ_{238}, λ_{235}, andλ_{232} are the respective decay constants, and t is the integration time in Ma.

Table 2: Unit-cell parameters of the BB zircon grains

Analysis	Unit-cell parameters	
	a_0 [Å]	c_0 [Å]
The α, β and γ angles are 90°.		
BB9-I	6.6152 ± 0.0006	6.0032 ± 0.0006
BB10	6.6144 ± 0.0003	6.0046 ± 0.0003
BB11	6.6142 ± 0.0003	6.0048 ± 0.0003
BB12-I	6.6147 ± 0.0004	6.0034 ± 0.0004
BB13	6.6185 ± 0.0004	6.0100 ± 0.0005
BB14	6.6144 ± 0.0003	6.0061 ± 0.0004
BB15	6.6072 ± 0.0005	5.9897 ± 0.0006
BB18	6.6141 ± 0.0003	6.0011 ± 0.0003

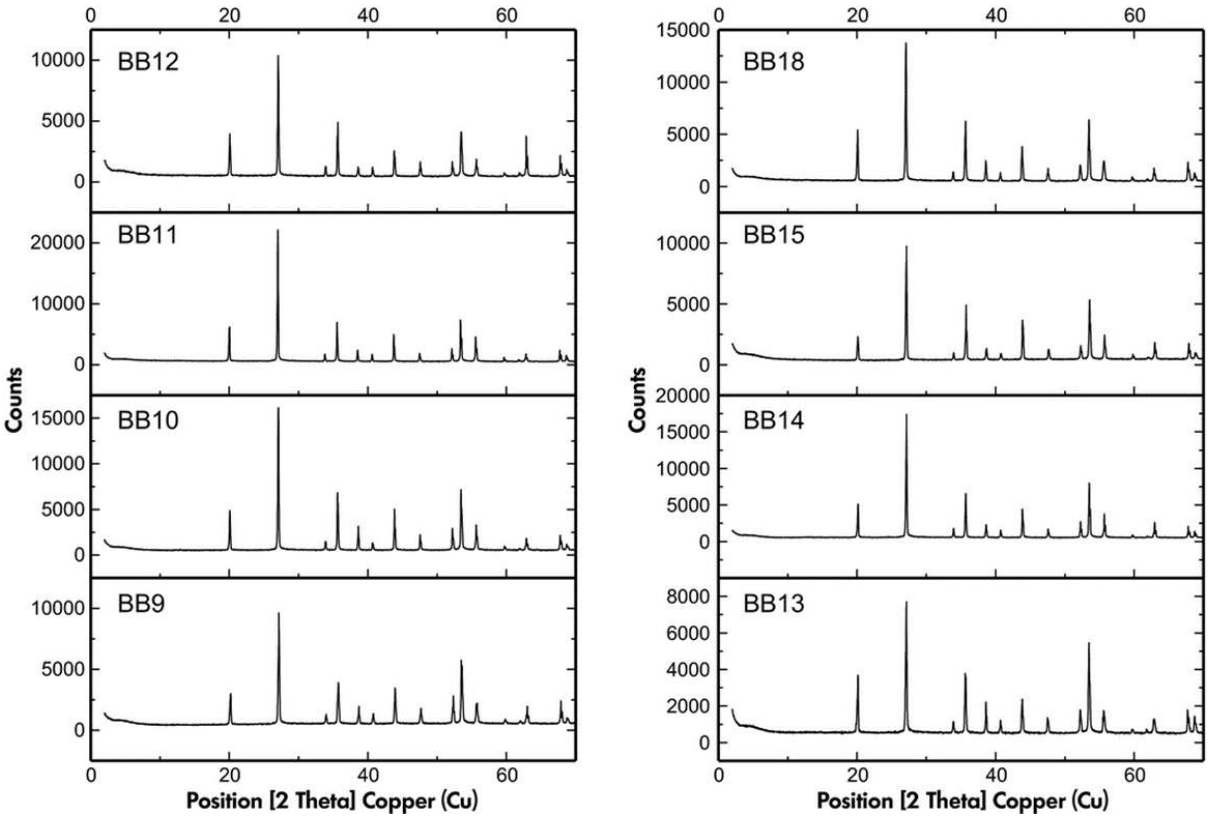

Figure 3: XRD patterns of eight zircon fragments with well-defined peaks and low background values, illustrating the good crystallinity of the BB zircon

The average calculated doseof0.59×10^{18} alpha-events per gram corresponds to a "well-crystallized" structure according to Murakami *et al.* (1991). The unit-cell parameters of BB zircon correspond well to this calculated alphadose. In addition, the data for BB zircons are within the trend of previously studied, untreated zircon samples from Sri Lanka, however they are slightly poorer in U and Th (discussed later).

The current degree of radiation damage in the zircons (Figure 4) was determined from the FWHM of the $\nu_3(SiO_4)$ Raman band (internal anti-symmetric stretching of SiO_4 tetrahedrons; B1g mode). This band was observed at 1001.6 ± 0.8 cm^{-1}, and its corrected FWHM was determined to be 7.2 ± 0.8 cm^{-1}. These values suggest a moderately mild radiation-damage state and as with most Sri Lankan zircons they likely experienced significant structural recovery through annealing (e.g., Nasdala et al., 2004)

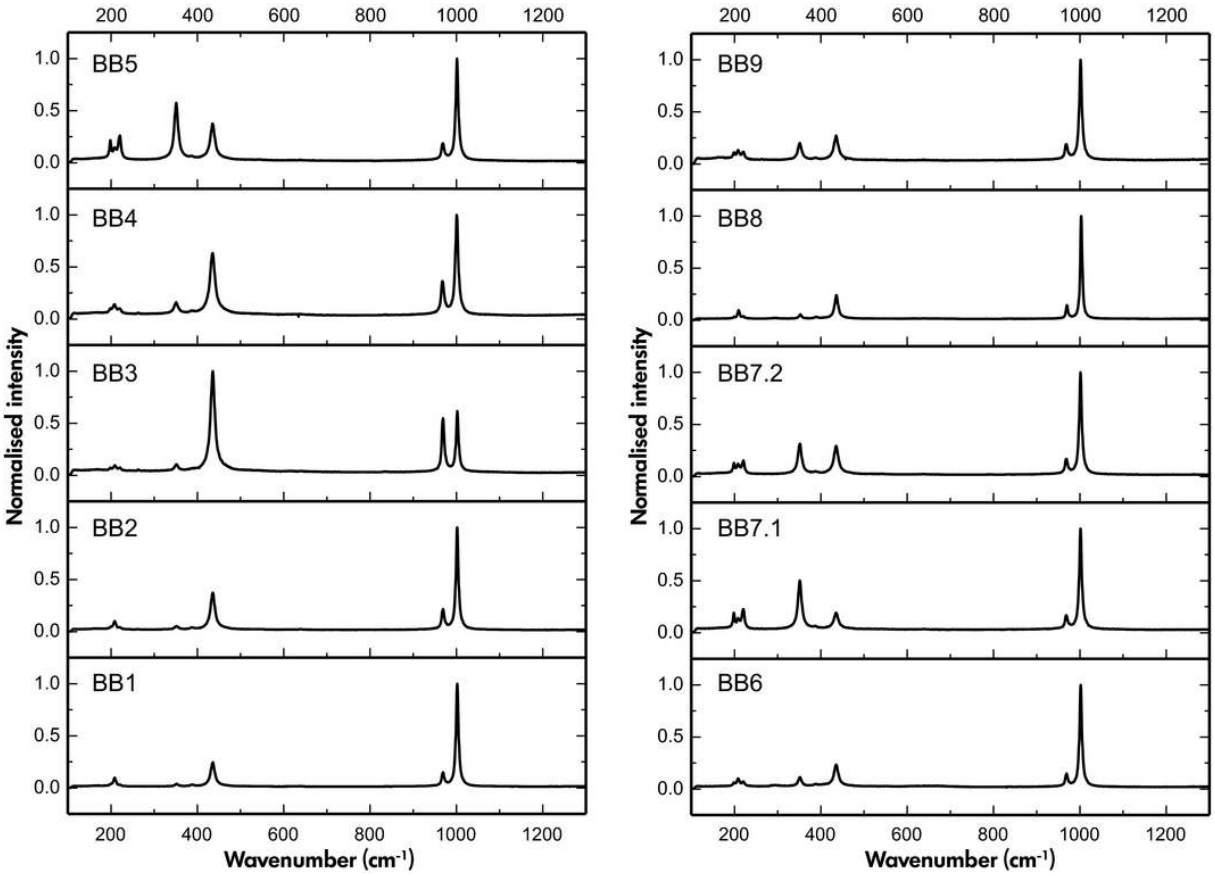

Figure 4: Raman spectra from nine fragments of BB zircon

Trace element and Hf mass fraction

The trace element and Hf mass fractions are presented in Tables3a and 3b and also in Figures 5 and 6. Although the individual fragments investigated here are homogeneous on a 10s of micron scale, the whole-grain analyses showed a small amount of internal variation, as can be seen in the REE patterns of homogeneous and fractured domains of BB zircons (Figure 6). This variation is observed only in some of the BB grains (e.g., BB17 and BB25) and relates to the CL-bright, fractured domains that returned slightly lower mass fractions in most REEs (Figure 6 and Table 3b) relative to nearby CL-dark domains. Trace element contents also differ slightly between different crystals. For example, the average U and radiogenic Pb contents vary between 227 and 368µg g^{-1}, and 2.1 and 7.9µg g^{-1}, respectively. The average Th/U ratio varies between 0.20 and 0.47 (based on the values presented in Table 3). Average mass fractions of

rare earth elements, such as Ce, Nd, Sm and Eu, vary between 1.3 and 2.3µg g^{-1}, 0.7 and 3.0µg g^{-1}, 0.7 and 4.6µg g^{-1} and 0.3 and 1.3µg g^{-1}, respectively. The REEs show steep chondrite normalized patterns enriched in HREE relative to LREE, small negative Eu and small positive Ce anomaly (La_N/Lu_Nvaries between 0.0025 – 0.0129, Eu/Eu* varies between 0.53 – 0.73, Ce/Ce* varies between1.46 – 2.83).

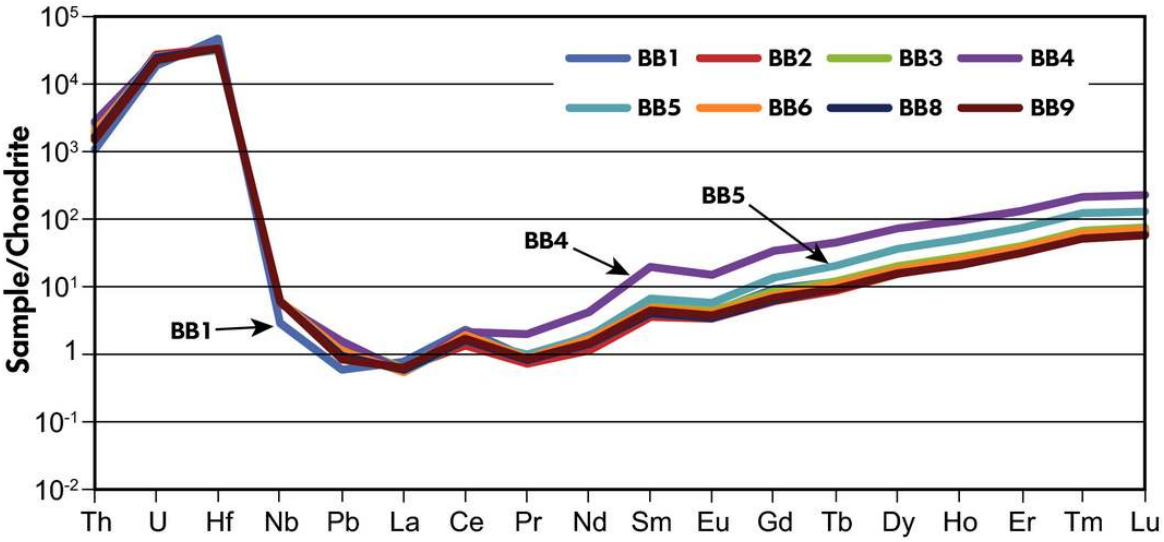

Figure 5: Chondrite-normalised trace element composition of eight fragments of the BB zircon (after Taylor and McLennan 1985).

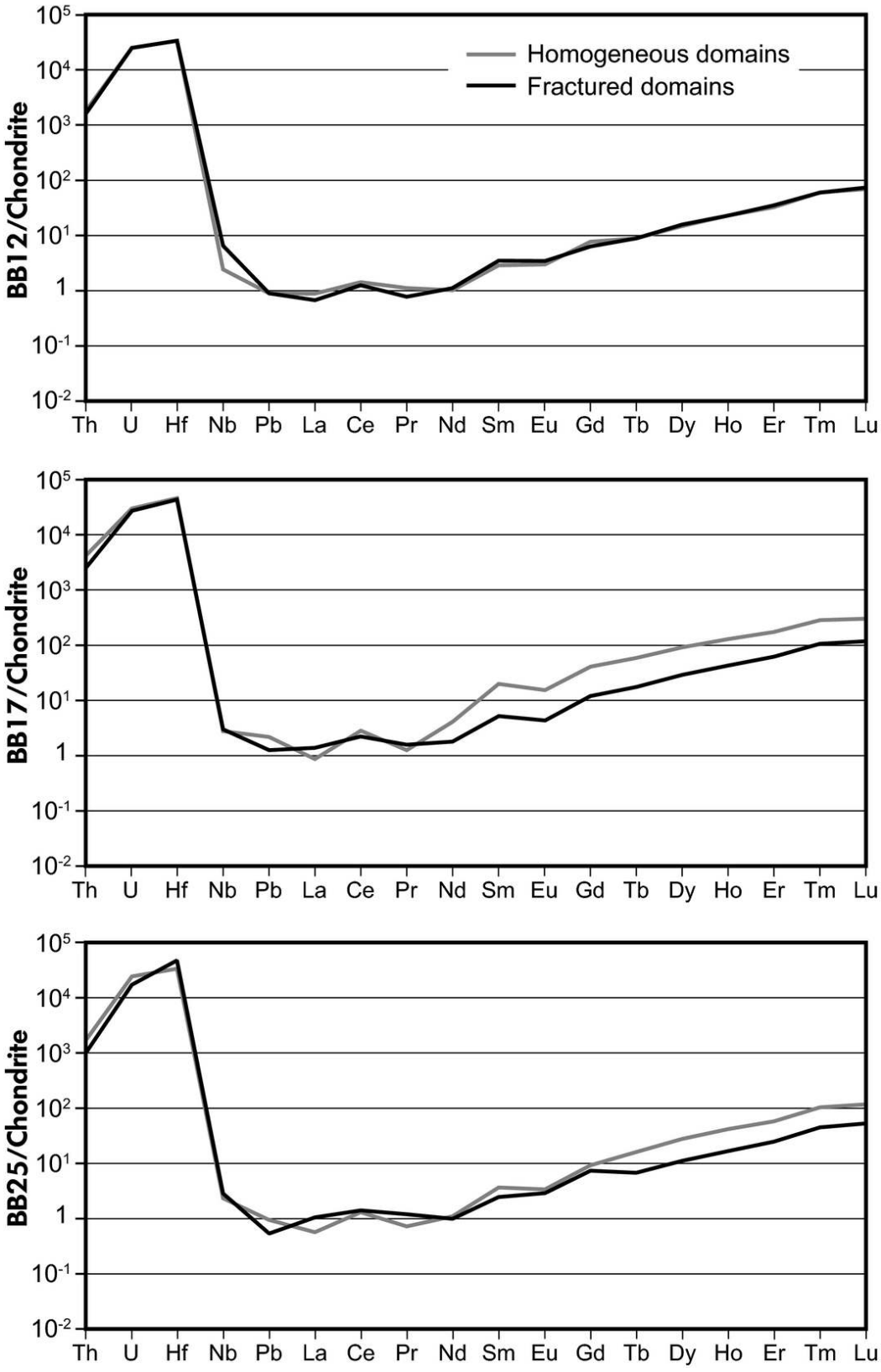

Figure 6: Comparison of the trace element compositions between homogeneous and fractured domains for three individual BB zircons

Table 3a: Average hafnium and trace element mass fractions of BB zircons

	Mass fractions (μg g^{-1}) ± 1*s* (*n* = 10)							
	BB1a	**BB2a**	**BB3a**	**BB4a**	**BB5a**	**BB6a**	**BB8a**	**BB9-Ia**
Nb	1.07 ± 0.04	2.22 ± 0.09	2.2 ± 0.07	2.1 ± 0.07	2.27 ± 0.06	2.28 ± 0.09	2.25 ± 0.07	2.26 ± 0.08
La	0.28 ± 0.01	0.22 ± 0.02	0.22 ± 0.01	0.21 ± 0.01	0.2 ± 0.02	0.2 ± 0.01	0.21 ± 0.02	0.23 ± 0.02
Ce	2.2 ± 0.09	1.28 ± 0.03	1.91 ± 0.04	2.04 ± 0.06	1.56 ± 0.04	1.82 ± 0.07	1.55 ± 0.08	1.62 ± 0.04
Pr	0.12 ± 0.003	0.1 ± 0.01	0.12 ± 0.01	0.27 ± 0.02	0.13 ± 0.01	0.12 ± 0.01	0.11 ± 0.01	0.12 ± 0.01
Nd	1.3 ± 0.1	0.8 ± 0.1	1.3 ± 0.1	3 ± 0.2	1.3 ± 0.1	1.2 ± 0.1	1 ± 0.1	1 ± 0.1
Sm	1.2 ± 0.3	0.8 ± 0.1	1.2 ± 0.1	4.5 ± 0.1	1.5 ± 0.1	1.1 ± 0.1	0.9 ± 0.1	1 ± 0.1
Eu	0.4 ± 0.04	0.3 ± 0.03	0.4 ± 0.02	1.3 ± 0.05	0.5 ± 0.04	0.4 ± 0.02	0.3 ± 0.02	0.3 ± 0.01
Gd	2.8 ± 0.4	1.9 ± 0.2	2.6 ± 0.3	10.4 ± 0.3	4.1 ± 0.3	2.3 ± 0.1	1.9 ± 0.1	2.1 ± 0.1
Tb	0.7 ± 0.04	0.5 ± 0.02	0.7 ± 0.04	2.6 ± 0.1	1.2 ± 0.04	0.6 ± 0.02	0.5 ± 0.03	0.5 ± 0.02
Dy	6.5 ± 0.3	5.8 ± 0.2	7.7 ± 0.4	27.6 ± 0.5	13.7 ± 0.5	6.8 ± 0.3	6 ± 0.2	5.9 ± 0.1
Ho	2 ± 0.1	1.8 ± 0.1	2.3 ± 0.1	8 ± 0.2	4.3 ± 0.2	2.1 ± 0.1	1.8 ± 0.04	1.8 ± 0.1
Er	8 ± 0.6	8 ± 0.3	10 ± 1	33 ± 0.5	18 ± 0.7	9 ± 0.5	8 ± 0.2	8 ± 0.2
Tm	1.93 ± 0.12	2.02 ± 0.07	2.39 ± 0.13	7.57 ± 0.14	4.35 ± 0.15	2.19 ± 0.09	1.83 ± 0.05	1.83 ± 0.04
Yb	71 ± 1.6	61 ± 1.9	64 ± 2	124 ± 2.6	85 ± 2.4	63 ± 1.6	58 ± 1.1	58 ± 1.7
Lu	2.5 ± 0.2	2.6 ± 0.1	2.9 ± 0.2	8.6 ± 0.1	4.9 ± 0.3	2.7 ± 0.1	2.2 ± 0.1	2.2 ± 0.04
Hf	8403 ± 118	6117 ± 99	5866 ± 71	5960 ± 106	5649 ± 161	6089 ± 105	5983 ± 66	6008 ± 112
Pb	2.1 ± 0.2	3.5 ± 0.1	5.1 ± 0.4	5.7 ± 0.1	3.9 ± 0.2	4.1 ± 0.2	3.4 ± 0.1	3.1 ± 0.1
Th	45 ± 2.1	71 ± 2.2	101 ± 6.7	116 ± 3.3	80 ± 2.6	84 ± 4.1	70 ± 1.2	63 ± 1.5
U	227 ± 13.9	332 ± 6.1	302 ± 8.3	292 ± 5.3	307 ± 9.6	280 ± 9.3	299 ± 4.7	270 ± 3.5
Th/U	0.2 ± 0.01	0.21 ± 0.005	0.33 ± 0.02	0.4 ± 0.01	0.26 ± 0.01	0.3 ± 0.01	0.23 ± 0.01	0.23 ± 0.004
La_N/Lu_N	0.0121 ± 0.0003	0.0089 ± 0.0005	0.008 ± 0.0003	0.0025 ± 0.0001	0.0042 ± 0.0003	0.0078 ± 0.0005	0.01 ± 0.001	0.0109 ± 0.0012
Ce/Ce*	2.78 ± 0.1	2.03 ± 0.13	2.79 ± 0.13	2.04 ± 0.06	2.25 ± 0.11	2.78 ± 0.15	2.36 ± 0.13	2.34 ± 0.12
Eu/Eu*	0.61 ± 0.1	0.73 ± 0.07	0.67 ± 0.04	0.58 ± 0.02	0.61 ± 0.04	0.68 ± 0.05	0.68 ±0.06	0.69 ± 0.04

Table 3b: Average hafnium and trace element mass fractions in homogeneous/fractured domains

	Mass fractions (µg g^{-1}) ± 1*s*					
	BB12a		**BB17a**		**BB25a**	
	Homogeneous	**Fractured**	**Homogeneous**	**Fractured**	**Homogeneous**	**Fractured**
Nb	0.87 ± 0.05	2.25 ± 0.05	1.03 ± 0.04	1.11 ± 0.05	0.83 ± 0.04	1 ± 0.07
La	0.32 ± 0.01	0.24 ± 0.02	0.31 ± 0.02	0.51 ± 0.04	0.21 ± 0.03	0.39 ± 0.03
Ce	1.39 ± 0.16	1.21 ± 0.05	2.77 ± 0.08	2.14 ± 0.08	1.27 ± 0.09	1.36 ± 0.06
Pr	0.15 ± 0.004	0.11 ± 0.01	0.17 ± 0.03	0.22 ± 0.02	0.1 ± 0.01	0.16 ± 0.01
Nd	0.7 ± 0.1	0.8 ± 0.1	2.9 ± 0.1	1.3 ± 0.1	0.8 ± 0.1	0.7 ± 0.1
Sm	0.7 ± 0.02	0.8 ± 0.1	4.6 ± 0.5	1.2 ± 0.2	0.9 ± 0.1	0.6 ± 0.03
Eu	0.3 ± 0.01	0.3 ± 0.02	1.3 ± 0.1	0.4 ± 0.1	0.3 ± 0.04	0.2 ± 0.01
Gd	2.4 ± 0.1	2 ± 0.1	12.5 ± 0.4	3.7 ± 0.9	2.9 ± 0.3	2.3 ± 0.1
Tb	0.5 ± 0.03	0.5 ± 0.02	3.4 ± 0.1	1 ± 0.4	0.9 ± 0.1	0.4 ± 0.04
Dy	5.8 ± 0.2	6.2 ± 0.2	34.7 ± 0.6	11.1 ± 4	10.6 ± 0.7	4.2 ± 0.2
Ho	2 ± 0.1	2 ± 0.1	10.9 ± 0.3	3.6 ± 1.4	3.6 ± 0.2	1.4 ± 0.1
Er	8 ± 0.3	9 ± 0.4	43 ± 1	15 ± 6	15 ± 0.7	6 ± 0.2
Tm	2.11 ± 0.04	2.15 ± 0.1	10.1 ± 0.45	3.75 ± 1.37	3.67 ± 0.18	1.6 ± 0.07
Yb	61 ± 1.1	63 ± 1.6	156 ± 4.6	88 ± 14.5	75 ± 2.2	70 ± 1.5
Lu	2.6 ± 0.1	2.8 ± 0.2	11.5 ± 0.3	4.5 ± 1.6	4.5 ± 0.2	2 ± 0.1
Hf	6160 ± 93	6193 ± 147	8276 ± 166	7895 ± 109	6071 ± 123	8634 ± 197
Pb	3.15 ± 0.15	3.21 ± 0.11	7.92 ± 0.37	4.6 ± 0.33	3.38 ± 0.4	1.92 ± 0.11
Th	77 ± 2.5	68 ± 2.4	174 ± 5.9	104 ± 5.5	73 ± 2.3	43 ± 1.3
U	311 ± 7	312 ± 11.6	368 ± 5.4	341 ± 3.8	296 ± 7.7	211 ± 5.4
Th/U	0.25 ± 0.01	0.22 ± 0.01	0.47 ± 0.01	0.3 ± 0.02	0.25 ± 0.01	0.2 ± 0.005
La_N/Lu_N	0.0129 ± 0.0008	0.0089 ± 0.0005	0.0028 ± 0.0002	0.0133 ± 0.0045	0.0048 ± 0.0006	0.0198 ± 0.0017
Ce/Ce*	1.46 ± 0.15	1.77 ± 0.15	2.83 ± 0.24	1.51 ± 0.13	2.11 ± 0.25	1.27 ± 0.09
Eu/Eu*	0.62 ± 0	0.73 ± 0.04	0.53 ± 0.03	0.54 ± 0.04	0.57 ± 0.06	0.67 ± 0.003
n	9	7	8	9	25	10

a LA-SF-ICP-MS data

U-Pb dating

Results of ID-TIMS U-Pb dating of different BB crystals are shown in Figure 7 and Appendix C - Supplementary data. The ID-TIMS data have a spread in $^{206}Pb/^{238}U$ and $^{207}Pb/^{206}Pb$ ages from *circa* 565 to 553 Ma and almost all analyses yield $^{206}Pb/^{238}U$ dates that are ~0.5% younger than $^{207}Pb/^{206}Pb$ dates, as is found within other high quality zircon reference materials of Early Paleozoic to Late Precambrian age (Schoene *et al.* 2006, Mattinson 2010). Each of the crystal fragments yielded approximately the same range of ages, from ~554 to ~563 Ma for $^{206}Pb/^{238}U$ and ~556 to ~565 Ma for $^{207}Pb/^{206}Pb$. To investigate the source of scatter in the $^{206}Pb/^{238}U$ and $^{207}Pb/^{206}Pb$ ages, we focus our discussion on the results on crystal BB9 that was analyzed in four independent TIMS laboratories (Table 4).

Table 4: Summary of ID-TIMS U-Pb and Pb-Pb data for the BB9 zircon

Laboratories	Pb_c(pg)	Atomic ratios							Apparent ages					
		Th/U	$^{206}Pb/^{238}U$	% RSD	$^{207}Pb/^{235}U$	% RSD	$^{207}Pb/^{206}Pb$	% RSD	$^{206}Pb/^{238}U$ (Ma)	% RSD	$^{207}Pb/^{235}U$ (Ma)	% RSD	$^{207}Pb/^{206}Pb$ (Ma)	% RSD
Uncertainty estimates are 2*s*.														
BSU (*n* = 12) CA-TIMS	0.65	0.24	0.0904 ± 0.0004	0.24	0.7331 ± 0.0048	0.33	0.0588 ± 0.00014	0.12	558 ± 2	0.2	558 ± 2	0.2	560 ± 4	0.4
NIGL (*n* = 8) CA-TIMS	0.63	0.33	0.0911 ± 0.0002	0.08	0.7401 ± 0.0012	0.09	0.0589 ± 0.00002	0.02	562 ± 0.8	0.1	562 ± 0.8	0.1	564 ± 0.8	0.1
JSGL (*n* = 3) CA-TIMS	7.95	0.22	0.0913 ± 0.0002	0.1	0.7421 ± 0.0020	0.14	0.0589 ± 0.00006	0.04	563 ± 1	0.1	564 ± 1.2	0.1	565 ± 2	0.2
Oslo (*n* = 3) ID-TIMS	2.54	0.32	0.0910 ± 0.0004	0.24	0.7391 ± 0.0044	0.29	0.0589 ± 0.00006	0.05	561 ± 2.6	0.2	561 ± 2	0.2	564 ± 2	0.2

We observed that some of the ages determined by CA-TIMS were similar to those reported by conventional ID-TIMS, and that the within-laboratory results from fragments of the same BB9 crystal (e.g., BB9-I, BB9-II, BB9-III, BB9-IV) record a smaller(0.1% to 0.4%)variation than between different crystal fragments (Figure 7c). The JSGL, NIGL, Oslo fragments yielded similar results within <1%, while the BSU aliquot gave younger dates within an internal 1% spread of results (Figure 7c).The BSU analyses also show broader scatter (0.4% RSD) than the other laboratories (0.2% RSD; Table 4), suggesting that the BB9-IV aliquot was detectably heterogeneous. Detailed SEM imaging at BSU revealed that some fragments contained dissolution features namely vermiform etch "tubes", which were created by the chemical abrasion process(Figure 7d, e).

We believe that these vermiform features are likely associated with dislocation tangles created during the long-lived Ratnapura metamorphic event (Kröner *et al.* 1994b, Dissanayake *et al.* 2000, Sajeev *et al.* 2010). The density of such features varies, but they are ubiquitous. Such fractures were preferentially etched during acid washing, suggesting that they are compositionally distinct in terms of low U and trace element contents, as indicated by the bright zoning of CL images(Figure 2) and trace element analyses (Table 3b). The same should apply for grains BB12 and BB17, which show a narrow spread in age for intra-laboratory crystal fragments (< 0.4%), but wide age variations (1-1.5%) for results from different labs and significantly different parent aliquots of the crystals (Figure7). The narrow spread in the intra-laboratory ages from the same parent aliquots suggests that the grains have highly homogenous domains, but that careful scrutiny may be required to identify these domains.

Further investigations on the isotopic heterogeneity were made by combining CL-imaging and LA-MC-ICP-MS (Laser Ablation Multi-Collector-Inductively Coupled Plasma-Mass Spectrometry) for BB9, BB17 and BB39. To ensure that the results were not affected by instrumental drift, we bracketed the analyses between analyses of two/three other reference materials (Figures 8 and 9). These three BB grains do not universally show strong, patchy CL zoning, but pits and fractures are visible that are interpreted as favorable sites for Pb loss (e.g. Cherniak and Watson, 2001) (e.g. Figure 2b). Some grains also show oscillatory zoning at their edges. Results of LA-MC-ICP-MS show clear

$^{206}Pb/^{238}U$ age variations between dark and bright patchy CL domains. The bright, patchy domains – commonly associated with dissolution pits – yield dates that average at 556 ± 5 Ma (2SD), 549 ± 7 Ma (2SD) and 548 ± 7 Ma(2SD), whereas homogeneous dark domains gave ages that are identical to older TIMS ages obtained for BB9, BB12 and BB17 (average at 561 ± 3 Ma (2SD) and 562± 3 Ma(2SD)).It is important to note that if CL/BSE and optical imaging are combined, it is possible to separate these domains during analysis.

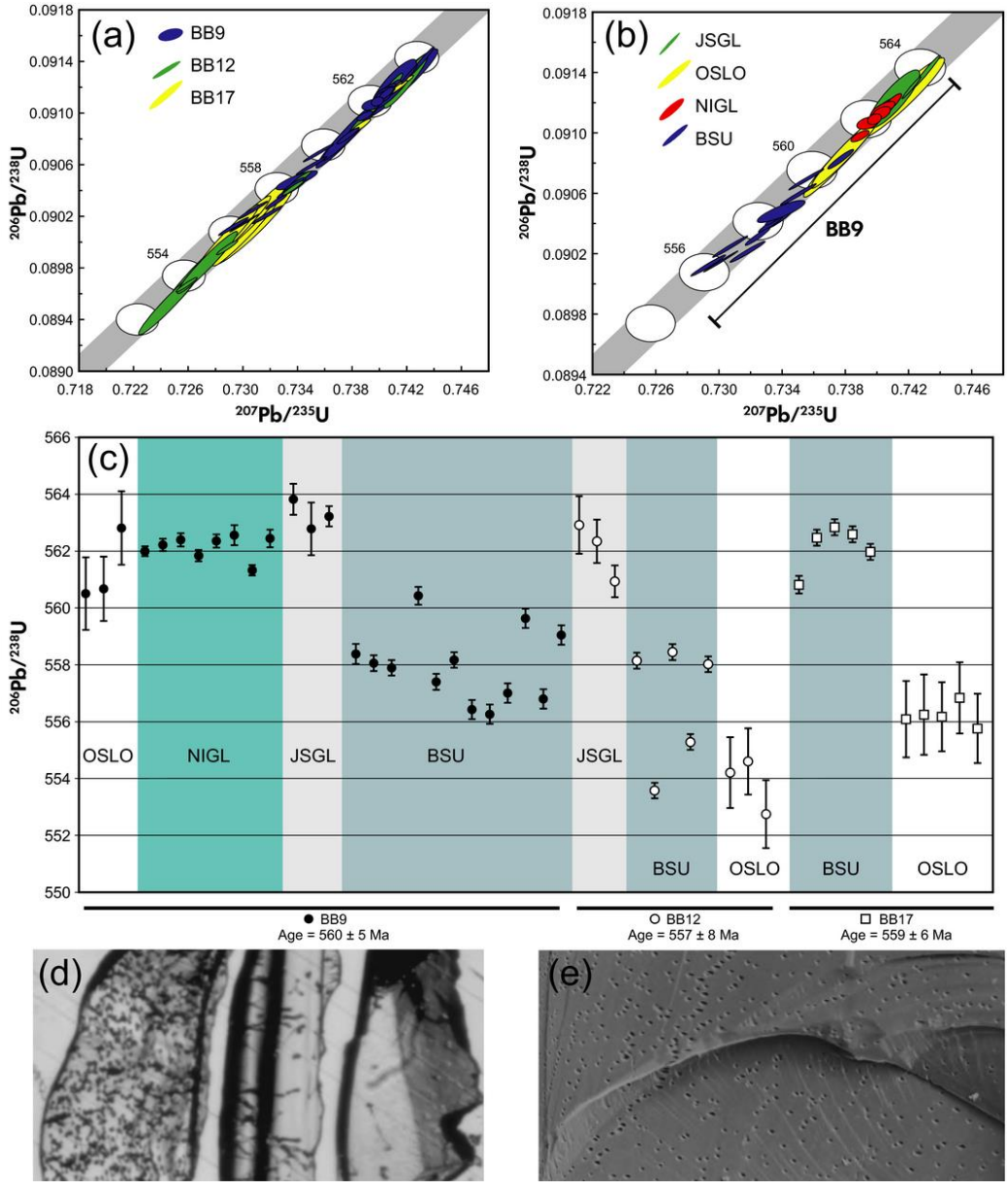

Figure 7: TIMS U-Pb dates of BB zircons: (a) Concordia diagram with all data collected from the Jack Satterly Geochronology Laboratory, NERC Isotope Geosciences Laboratory, University of Oslo and Boise State University. (b) Concordia diagram with all data points for crystal BB9 from the different laboratories. (c) Average 206Pb/238U mean dates showing the spread in ages obtained in four TIMS laboratories. (d) Transmitted and (e) BSE images of small fragments of BB showing micrometre-scale dissolution pits and tube-like features.

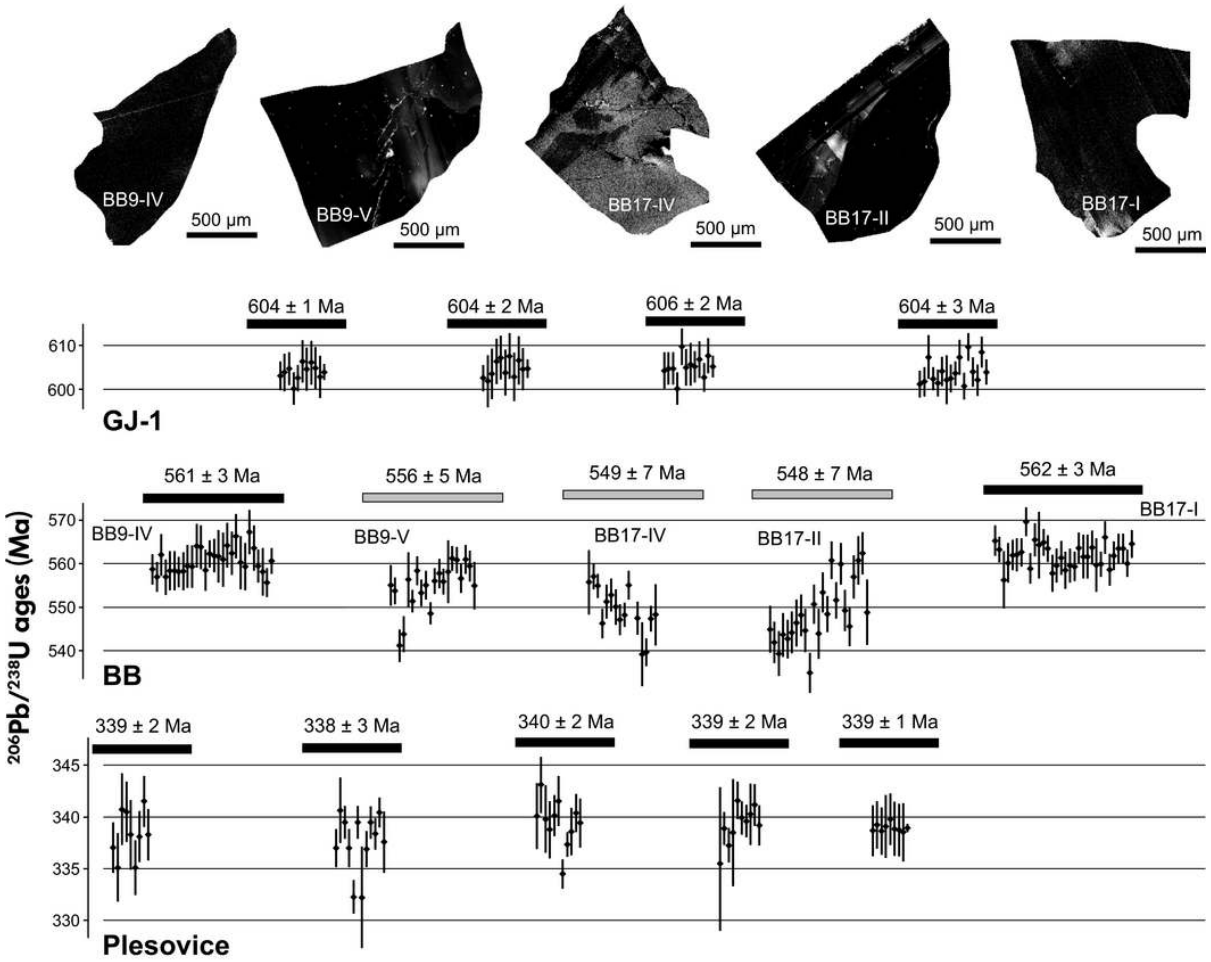

Figure 8: Cathodoluminescence images (top) of fragments, showing some patchy domains, and LA-MC-ICP-MS U-Pb dates (obtained at UFOP) of BB, GJ-1 and Plešovice zircon reference materials. Grey bars for BB fragments correspond to bright, patchy domains in fragments BB9-V, BB17-IV and BB17-II, whereas black bars are for BB9-IV and BB17-I. Error bars are 2 s.

Spot analyses on BB39 were targeted at fractured domains and oscillatory rims. Surprisingly, the oscillatory rims gave identical dates to those yielded by homogeneous domains with an average $^{206}Pb/^{238}U$ date of 560 ± 3Ma (2SD). Analyses on fractured domains gave a slightly younger $^{206}Pb/^{238}U$ age of 556 ± 4 Ma (2SD). This shows that each BB megacrysts can produce a number of isotopically homogeneous fragments, suitable for use as either primary calibration or quality control materials. These results also show that heterogeneities in the U-Th-Pb system can be detected by careful CL imaging in an analogous manner to the identification and avoidance of domains in other U-Pb reference materials, as in Plešovice zircon, which has U- and Th-rich domains that appear as bright patches on BSE images (Sláma *et al.*2008).

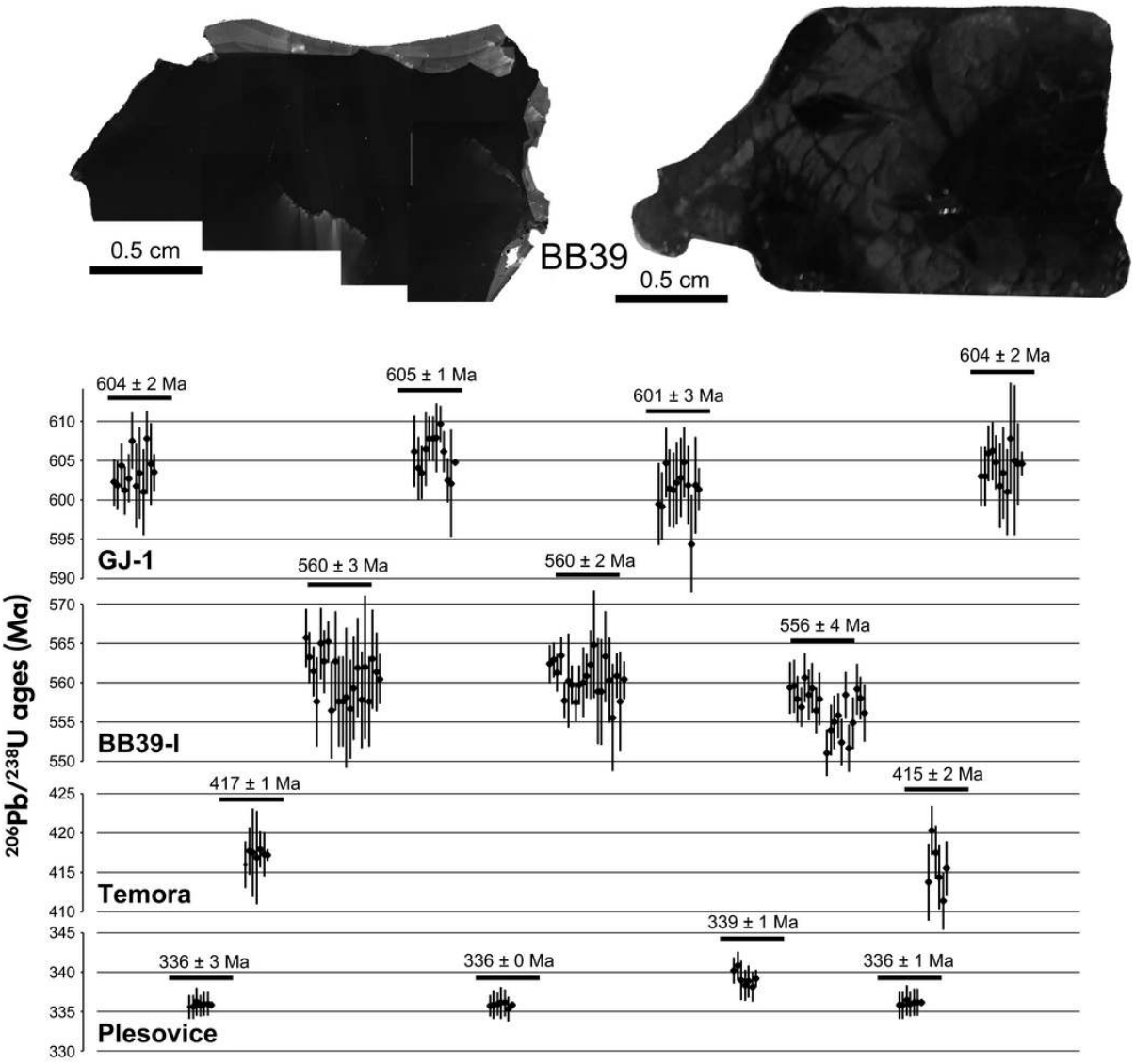

Figure 9: Whole-grain imaging via cathodoluminescence (top left) and transmitted light (top right), and LA-MC-ICP-MS U-Pb dates (obtained at the Federal University of Ouro Preto) for BB39, GJ-1, Temora and Plešovice zircon reference materials. Uncertainty estimates are 2s

Inter-laboratory comparisons that focused on dating unaltered, CL-dark domains from BB zircons from six different LA-ICP-MS instruments yielded identical results within the limits of the reported analytical uncertainty(Tables 5a-c and Figure 10). For instance, the calculated laser ablation ICP-MS ages determined at UFOP, JWG, USP and University of Portsmouth are as follows (for individual analyses, see Appendix C - Supplementary data): by LA-Q-ICP-MS – 563 ± 31 Ma ($^{207}Pb/^{206}Pb$), 562 ± 4 Ma ($^{206}Pb/^{238}U$) and 562 ± 5 Ma ($^{207}Pb/^{235}U$) (2SD,92 analyses in 7 BB zircons, UFOP, Figure 10a; Table 5a), by LA-SF-ICP-MS– 562 ± 10Ma ($^{207}Pb/^{206}Pb$), 562 ± 9 Ma ($^{206}Pb/^{238}U$) and 562 ± 7 Ma ($^{207}Pb/^{235}U$) (2SD,193 analyses in 8 BB zircons, UFOP, Figure 10c; Table 5b), by

LA-MC-ICP-MS – 564 ± 7 Ma ($^{207}Pb/^{206}Pb$), 560 ± 6 Ma ($^{206}Pb/^{238}U$) and 561 ± 6 Ma ($^{207}Pb/^{235}U$) (2SD, 93 analyses in 3 BB zircons, UFOP, Figure 10e; Table 5c); 561 ± 9 Ma ($^{207}Pb/^{206}Pb$), 562 ± 6 Ma ($^{206}Pb/^{238}U$) and 562 ± 5 Ma ($^{207}Pb/^{235}U$) (2SD,114 analyses in 10 BB zircons, JWG, Figure 10d; Table 5b);570 ± 61 Ma ($^{207}Pb/^{206}Pb$), 562 ± 9 Ma ($^{206}Pb/^{238}U$) and 564 ± 16 Ma ($^{207}Pb/^{235}U$) (2SD, 112 analyses in 3 BB zircons, USP, Figure 10f; Table 5c); and 567 ± 44 Ma ($^{207}Pb/^{206}Pb$), 562 ± 22 Ma ($^{206}Pb/^{238}U$) and 558 ± 16 Ma ($^{207}Pb/^{235}U$) (2SD, 30 analyses in one BB zircon, University of Portsmouth, Figure 10b; Table 5a).

Thus we conclude that fragments BB crystals marked by CL-dark and which are weakly zoned in BSE imaging are isotopically homogeneous and record identical ages at the level of precision documented by hundreds of laser ablation analyses (e.g., Figure10). Because the BB grains are large (>1cm),domains within the mega crystals may record younger ages, which in the cases of BB9, BB12 and BB17 resulted in a 9-10 Ma spread in ID-TIMS dates. Nevertheless, these domains can be easily avoided using detailed CL-imaging and some LA-MC-ICP-MS U-Pb dating prior to distribution.

Judging from the great number of ID-TIMS analyses obtained here, the BB zircon group is considered one of the best characterized reference material for LA-ICP-MS geochronology (Table 6a), in the sheer number of discrete analyses across laboratories that have been undertaken. The BB suite is also one of the most abundant materials for distributing to LA-ICP-MS laboratories. BB grains show similar U and Pb mass fractions to those reported for the GJ-1 and Plešovice reference materials, and it has substantially greater Hf mass fractions than other reference materials (Table 6a). All analyzed fragments showed low levels of common Pb and high uranium and radiogenic Pb mass fractions , yielding high count rates and good counting statistics. If all TIMS ages are considered, the BB12, BB9 and BB17 show a 1-2% (10 Ma)spread in $^{206}Pb/^{238}U$ ages (47 TIMS analyses) that is slightly larger(within a ± 1 Ma uncertainty of apparent ages) than that published for GJ-1 (7 Ma – based on 8 ID-TIMS analyses; Jackson *et al*., 2004) and for 91500 (7 Ma – 11ID-TIMS analyses; Wiedenbeck *et al.* 1995).However, the spread in ages can be reduced (< 0.8% - 4 Ma) if the dates for the individual domain types are considered. Table 6b shows averaged results of TIMS values

recommend for the homogenous domains after CL imaging of individual fragments. We advise that, if constraints better than 1% are required for the use of the material, the distributed fragments should be analyzed by ID-TIMS for better constraints on uncertainty propagation. It is important to note that different geological analyses require different levels of precision, in other words, in the case of analyzes that do not require the highest level of accuracy (e.g., detrital zircon studies), BB zircon can be completely suitable as characterized in this work. However, if further information is required, then, ID-TIMS might be needed.

Table 5a: Summary of laser ablation Q-ICP-MS U-Pb data for BB zircon fragments

Analysis	Atomic ratios						Apparent ages (Ma)					
	$^{207}Pb/^{235}U$	2*s*(abs)	$^{206}Pb/^{238}U$	2*s*(abs)	$^{207}Pb/^{206}Pb$	2*s*(abs)	$^{207}Pb/^{235}U$	2*s*(abs)	$^{206}Pb/^{238}U$	2*s*(abs)	$^{207}Pb/^{206}Pb$	2*s*(abs)
UFOP BB9 (*n* = 12)	0.7415	0.0099	0.0912	0.0008	0.0590	0.0010	563	6	562	5	568	37
UFOP BB11 (*n* = 11)	0.7382	0.0099	0.0909	0.0009	0.0589	0.0010	561	6	561	5	565	37
UFOP BB12 (*n* = 15)	0.7395	0.0083	0.0911	0.0006	0.0589	0.0007	562	5	562	3	564	26
UFOP BB13 (*n* = 14)	0.7401	0.0056	0.0911	0.0009	0.0589	0.0006	562	4	562	5	565	23
UFOP BB14 (*n* = 14)	0.7402	0.0095	0.0911	0.0007	0.0590	0.0009	562	6	562	4	565	32
UFOP BB16 (*n* = 13)	0.7368	0.0130	0.0911	0.0005	0.0587	0.0010	561	8	562	3	556	38
UFOP BB17 (*n* = 13)	0.7380	0.0069	0.0910	0.0009	0.0588	0.0007	561	4	562	5	560	25
UFOP ALL (*n* = 92)	0.7392	0.0090	0.0911	0.0008	0.0589	0.0008	562	5	562	4	563	31
Portsmouth BB9 (*n* = 30)	0.7334	0.0269	0.0911	0.0037	0.0590	0.0012	558	16	562	22	567	44

Table 5b: Summary of laser ablation SF-ICP-MS U-Pb data for BB zircons

Summary	Atomic ratios						Apparent ages (Ma)					
	$^{207}Pb/^{235}U$	2*s*	$^{206}Pb/^{238}U$	2*s*	$^{207}Pb/^{206}Pb$	2*s*	$^{207}Pb/^{235}U$	2*s*	$^{206}Pb/^{238}U$	2*s*	$^{207}Pb/^{206}Pb$	2*s*
JWG BB1 (*n* = 8)	0.7392	0.0059	0.0912	0.0005	0.0588	0.0002	562	3	563	4	560	4
JWG BB2 (*n* = 5)	0.7411	0.0078	0.0913	0.0009	0.0589	0.0002	563	4	563	5	564	5
JWG BB3 (*n* = 14)	0.7389	0.0088	0.0911	0.0010	0.0588	0.0002	562	5	562	6	560	4
JWG BB4 (*n* = 6)	0.7408	0.0097	0.0913	0.0010	0.0588	0.0002	563	6	563	6	561	5
JWG BB5 (*n* = 11)	0.7378	0.0132	0.0910	0.0014	0.0588	0.0002	561	8	562	8	559	7
JWG BB6 (*n* = 10)	0.7391	0.0068	0.0912	0.0007	0.0588	0.0001	562	4	563	4	559	4
JWG BB8 (*n* = 5)	0.7369	0.0064	0.0910	0.0007	0.0588	0.0001	561	4	561	4	558	5
JWG BB9. (*n* = 21)	0.7426	0.0147	0.0913	0.0010	0.0590	0.0008	564	9	563	6	568	29
JWG BB16 (*n* = 29)	0.7394	0.0142	0.0910	0.0016	0.0589	0.0006	562	8	562	10	564	23
JWG BBF (*n* = 5)	0.7376	0.0066	0.0910	0.0007	0.0588	0.0001	561	4	561	4	559	4
JWG ALL (114)	0.7393	0.0094	0.0911	0.0010	0.0588	0.0003	562	5	562	6	561	9
UFOP BB9 (*n* = 33)	0.7379	0.0129	0.0909	0.0014	0.0589	0.0004	561	7	561	8	562	11
UFOP BB10 (*n* = 18)	0.7416	0.0100	0.0913	0.0011	0.0589	0.0002	563	8	563	9	565	11
UFOP BB11 (*n* = 20)	0.7373	0.0136	0.0908	0.0018	0.0589	0.0002	561	8	560	11	563	9
UFOP BB12 (*n* = 24)	0.7383	0.0109	0.0909	0.0014	0.0589	0.0004	561	6	561	8	563	14
UFOP BB13 (*n* = 19)	0.7401	0.0095	0.0911	0.0013	0.0589	0.0004	562	6	562	8	566	14
UFOP BB14 (*n* = 20)	0.7365	0.0127	0.0913	0.0016	0.0585	0.0001	561	8	563	10	550	4
UFOP BB16 (*n* = 35)	0.7410	0.0118	0.0912	0.0014	0.0589	0.0003	563	7	563	8	564	9
UFOP BB17 (*n* = 24)	0.7423	0.0106	0.0914	0.0012	0.0589	0.0001	564	6	564	7	565	5
UFOP ALL (193)	0.7394	0.0115	0.0911	0.0014	0.0589	0.0003	562	7	562	9	562	10

Table 5c: Summary of laser ablation MC-ICP-MS U-Pb data for BB zircons

Summary	Atomic ratios						Apparent ages (Ma)					
	$^{207}Pb/^{235}U$	2*s*	$^{206}Pb/^{238}U$	2*s*	$^{207}Pb/^{206}Pb$	2*s*	$^{207}Pb/^{235}U$	2*s*	$^{206}Pb/^{238}U$	2*s*	$^{207}Pb/^{206}Pb$	2*s*
UFOP BB9-I (*n* = 9)	0.7378	0.0116	0.0908	0.0011	0.0590	0.0002	561	7	560	7	566	7
UFOP BB12-I (*n* = 24)	0.7376	0.0084	0.0908	0.0009	0.0589	0.0002	561	5	560	5	564	7
UFOP BB39.1 (*n* = 60)	0.7349	0.0124	0.0906	0.0012	0.0588	0.0002	559	7	559	7	561	8
UFOP ALL (*n* = 93)	0.7368	0.0108	0.0907	0.0011	0.0589	0.0002	561	6	560	6	564	7
USP BB9 (*n* = 39)	0.7420	0.0237	0.0910	0.0016	0.0592	0.0014	564	14	561	9	573	54
USP BB12 (*n* = 35)	0.7479	0.0277	0.0914	0.0016	0.0594	0.0017	567	16	564	10	581	62
USP BB17 (*n* = 38)	0.7377	0.0299	0.0911	0.0014	0.0588	0.0018	561	17	562	8	558	69
USP ALL (*n* = 112)	0.7425	0.0271	0.0911	0.0016	0.0591	0.0017	564	16	562	9	570	61

For key to measurement laboratories see footnote to Table 1 and main text. Table 4 individual analyses are reported in online supporting information.

Table 6a: Summary of zircon reference material data

Reference material		Number of ID-TIMS analyses		Number of ID-TIMS laboratories	Number of crystals analysed by ID-TIMS	$^{206}Pb/^{238}U$ ID-TIMS age (Ma)	U (μg g^{-1})		Pb_{rad} (μg g^{-1})		Hf (μg g^{-1})		Grain size	Reference
91500		11		3	1	1059.2–1065.5	71–86		13–16		5610–29748		238 g	Wiedenbeck *et al.* (1995), Griffin *et al.* (2006)
GJ-1		8		1	4	596.2–602.7	212–422		19.3–37.4		~ 6558		*ca.* 1 cm	Jackson *et al.* (2004), Morel *et al.* (2008)
M257		34		4	1	559.3–564.1	812–863		52.0–90.1				19.5 mm	Nasdala *et al.* (2008)
Temora		21		1	3	415.25–417.82	60–600		~ 14.3		~ 8310		0.05–0.3 mm	Black *et al.* (2003, 2004)
Plešovice		27		5	7	336.15–337.70	465–3084		21–158		8980–14431		1–6 mm	Sláma *et al.* (2008)
BB	BB9	47	26	4	3	556–564	227–368	263–275	2.1–7.9	2.9–3.4	5649–8403	5793–6129	Up to 1 cm; ~300 g	This work
	BB12		11	3		553–563		302–321		2.9–3.4		5979–6321		
	BB17		10	2		556–563		361–378		7.5–8.6		8052–8592		

Table 6b: Recommended values for the BB zircon reference materials

Sample	Pb_c(pg)[a]	Atomic ratios								Apparent ages (Ma)					
		Th/U[b]	$^{206}Pb/^{204}Pb$[c]	$^{207}Pb/^{235}U$[d]	± (%)[e]	$^{206}Pb/^{238}U$[d]	± (%)[e]	$^{207}Pb/^{206}Pb$[d]	± (%)[e]	$^{207}Pb/^{235}U$[f]	±[g]	$^{206}Pb/^{238}U$[f]	±[g]	$^{207}Pb/^{206}Pb$[f]	±[g]
BB9 (n = 26)	1.70	0.27	75613.27	0.736983	0.000868	0.090797	0.000073	0.058867	0.000032	561	0.5	560	0.4	562	1.2
BB12 (*n* = 11)	1.99	0.30	112764.82	0.732341	0.001073	0.090313	0.000113	0.058767	0.000030	558	0.6	557	0.7	560	1.0
BB17 (*n* = 10)	2.45	0.22	122288.40	0.735291	0.001329	0.090616	0.000134	0.058850	0.000034	560	0.8	559	0.8	562	1.3

a Total mass of common Pb. b Th contents calculated from radiogenic 208Pb and the 207Pb/206Pb date of the sample, assuming concordance between U-Th and Pb systems. cMeasured ratio corrected for fractionation and spike contribution only. d Corrected for fractionation, spike and blank. All common Pb was assumed to be procedural blank. 206Pb/238U ratio corrected for initial disequilibrium in 230Th/238U using Th/U [magma] = 4 ± 1. e Uncertainties are 2s, propagated using the algorithms of Schmitz and Schoene (2007) and Crowley et al. (2007). f Calculations are based on the decay constants of Jaffey et al. (1971). 206Pb/238U date corrected for initial disequilibrium in 230Th/238U using Th/U [magma] = 4 ± 1. g Errors are 2s.

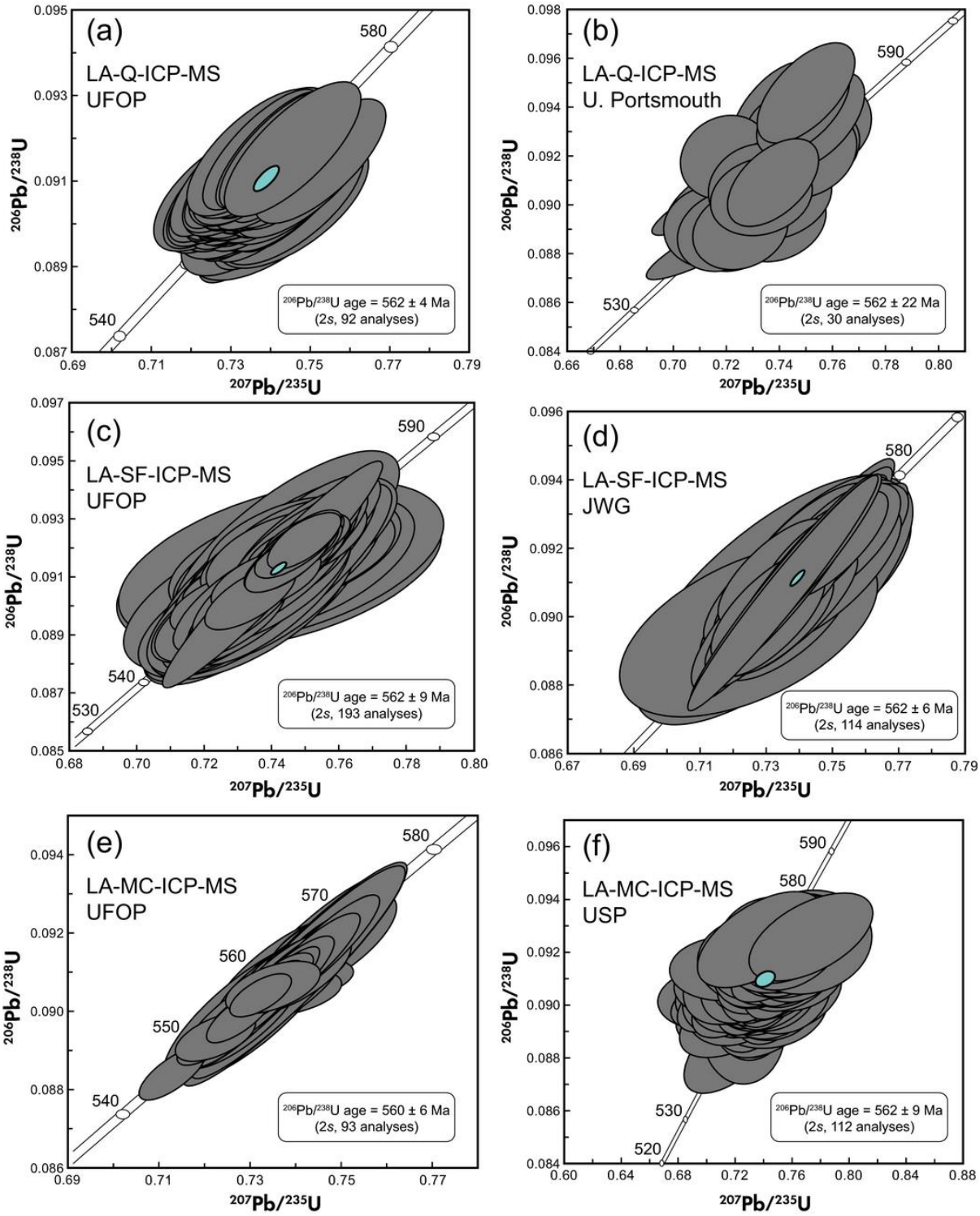

Figure 10: Laser ablation ICP-MS U-Pb ages obtained using: (a) Q-ICP-MS – Federal University of Ouro Preto (UFOP), (b) Q-ICP-MS – University of Portsmouth, (c) SF-ICP-MS – UFOP, (d) SF-ICP-MS – J.W. Goethe University of Frankfurt am Main, (e) MC-ICP-MS – UFOP and (f) MC-ICP-MS – University of São Paulo

The performance of the BB9 zircon as a primary reference material for laser ablation ICP-MS analysis was assessed via laser ablation SF-ICP-MS measurements of four other zircon reference materials, namely, Plešovice, M127 (Nasdala *et al.* 2016), GJ-1 and 91500. The analyses were calibrated against the BB9 crystal. Table 7 shows data obtained for the other zircon reference materials, using BB9 as primary calibrant and assuming 562 Ma ($^{207}Pb/^{206}Pb$), 560 Ma ($^{206}Pb/^{238}U$) and 561 Ma ($^{207}Pb/^{235}U$) (mean of TIMS ages; Table 4).The analyses of these reference materials using BB9 as calibrant in each case returned Concordia ages that were well within analytical uncertainty of the accepted age of the reference materials(Table 7). Problems in the analysis of the other zircon reference materials(as for instance irregular sputtering behavior, high ^{204}Pb count rates, U-Pb discordance) were not observed. Therefore, there appear to be no performance problems that would preclude the use of the BB9 zircon as a primary calibrant for laser ablation ICP-MS. In addition, at University of Portsmouth a small amount of data were collected using BB9 as primary reference material. In this arrangement, 91500 yielded $^{206}Pb/^{238}U$ and $^{207}Pb/^{206}Pb$ ages of 1065±59 Ma and 1063±56 Ma (n = 3, 2SD), respectively, that are consistent with published values.

Table 7: Results of laser ablation SF-ICP-MS U-Pb analyses of other zircon reference materials when calibrated *versus* BB zircon

Sample	Published age (Ma)	*n*	Determined age[a] when calibrated *versus* BB9 zircon		
			$^{207}Pb/^{235}U$	$^{206}Pb/^{238}U$	$^{207}Pb/^{206}Pb$
Plešovice	337	17	337 ± 1	337 ± 1	341 ± 13
M127	524	16	524 ± 3	524 ± 3	525 ± 12
GJ1	608	19	609 ± 2	607 ± 2	618 ± 13
91500	1065	12	1072 ± 7	1066 ± 5	1084 ± 23

a Calculated ages are weighted mean values. Uncertainties are quoted at the 95% confidence level; they include the uncertainty of the reference analyses.

Hf isotopic composition

The Hf mass fraction of the different BB zircon grains varies between 0.56 and 0.84 g/100g (Table3).Laser ablation MC-ICP-MS data suggest a homogenous Hf-isotope composition (Figure 11) both within and between individual zircon grains. A mean of Lu/Hf of 0.00008 and of $^{176}Hf/^{177}Hf$ for the pooled data set of0.281674 ± 0.000018 (2SD, 197 analyses from 16 grains) were measured. For reference zircons,$^{176}Hf/^{177}Hf$ values of0.28167±0.00002 (2SD)and $^{178}Hf/^{177}Hf$values of1.46720±0.00004(2SD) were obtained on JWG and$^{176}Hf/^{177}Hf$ values of 0.28168± 0.00001(2SD) and $^{178}Hf/^{177}Hf$ values of1.46726 ± 0.00001 (2SD) were obtained on UFOP (Table 8 – for individual analyses, see Appendix D - Supplementary data), and with a mean$^{176}Hf/^{177}Hf$ for the pooled data set of0.281674 ± 0.000018 (2SD,197analyses from 16grains).

The laser ablation Hf-isotope data obtained from the two laboratories are identical within analytical uncertainty, showing only a negligible difference in the results obtained for JWG and UFOP. The Hf-isotope composition of the studied zircons measured at the JWG shows somewhat large variation of the $^{176}Hf/^{177}Hf$ ratios within, and between, individual grains (cf. Figure 11). This might suggest some minor inter- and intra-grain heterogeneity of the Hf-isotope composition may have been detected at JWG. However, we suspect that the reported variations relate to the amount of material sampled during laser ablation, given that the laser conditions (spot size and energy) were different between the two laboratories. For instance at JWG spot sizes were substantially smaller (40 μm spots) than at UFOP (50 μm spots). This difference translated into much smaller uncertainty estimates for single measurements at UFOP, whereas the mean values remained essentially the same.

The BB zircon grains have an average ε_{Hf}(at 561 Ma)for the pooled data set of -26.9±0.6(2SD, Figure 11).All grains were marked by low Lu/Hf (averages of 0.00006 and 0.00009) and Yb/Hf (averages of 0.000004 and 0.000005) ratios. Further assessment of the

suitability of BB zircons as a reference material for Hf isotope analysis will require solution MC-ICP-MS data, which are beyond the scope of this contribution.

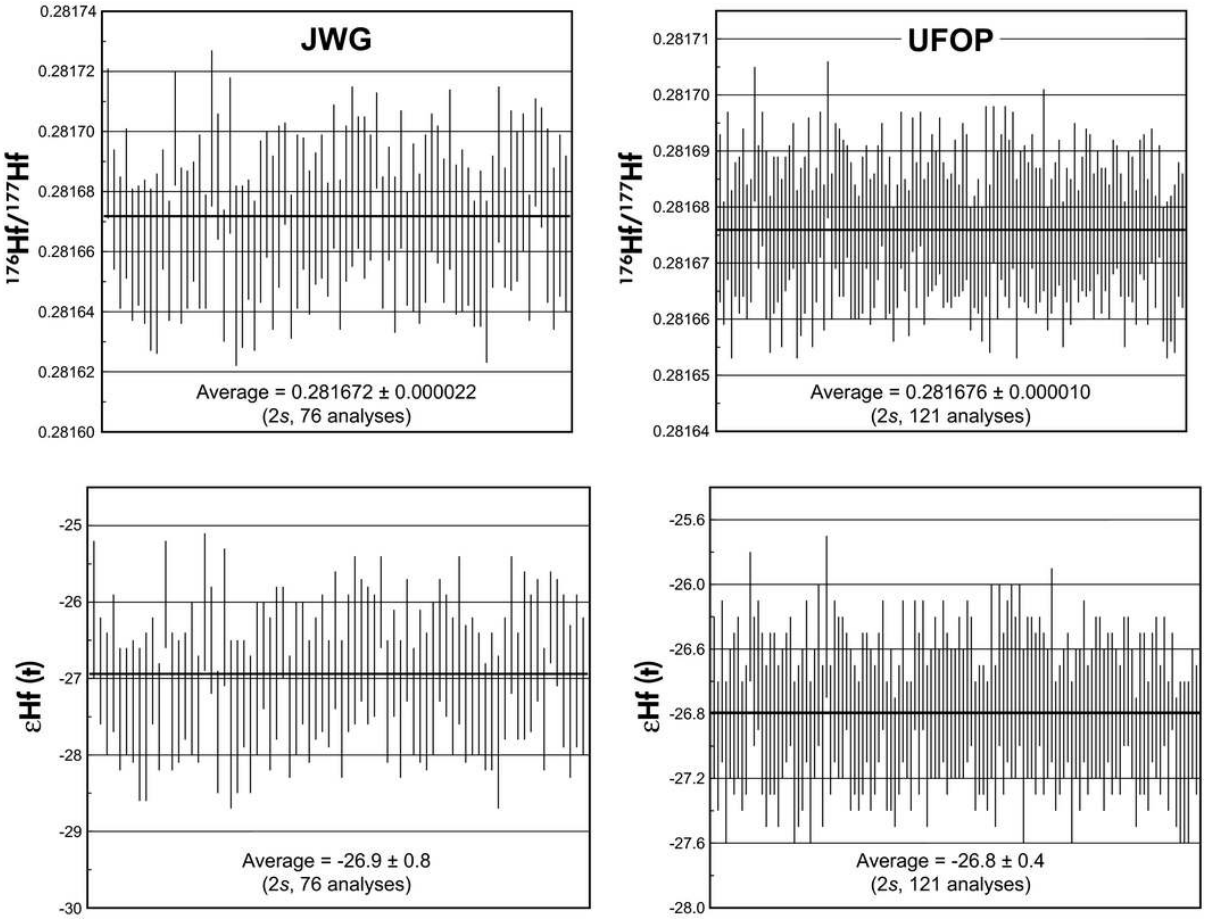

Figure 11: Hf isotope composition of the BB zircon samples obtained by laser ablation MC-ICP-MS analyses

Table 8: Summary of laser ablation MC-ICP-MS measurements of Hf isotope composition in the BB zircon

Analysis	Lu/Hf	Yb/Hf	$^{176}Hf/^{177}Hf$	2*s*	$^{178}Hf/^{177}Hf$	$^{180}Hf/^{177}Hf$	εHf_{561}	2*s*
JWG BB1 (*n* = 7)	0.00003	0.000002	0.281670	0.000027	1.46719	1.88663	−27.0	0.9
JWG BB2 (*n* = 13)	0.00015	0.000009	0.281670	0.000033	1.46720	1.88675	−27.1	1.2
JWG BB3 (*n* = 20)	0.00006	0.000004	0.281669	0.000023	1.46719	1.88676	−27.0	0.8
JWG BB4 (*n* = 5)	0.00005	0.000003	0.281684	0.000016	1.46721	1.88663	−26.5	0.6
JWG BB5 (*n* = 16)	0.00006	0.000004	0.281669	0.000018	1.46719	1.88682	−27.0	0.7
JWG BB6 (*n* = 5)	0.00004	0.000002	0.281668	0.000029	1.46723	1.88683	−27.1	1.0
JWG BB7 (*n* = 7)	0.00004	0.000002	0.281678	0.000023	1.46718	1.88676	−26.7	0.8
JWG BB9 (*n* = 3)	0.00005	0.000003	0.281666	0.000011	1.46723	1.88683	−27.1	0.4
JWG BB ALL	0.00006	0.000004	0.281672	0.000022	1.46720	1.88675	−26.9	0.8
UFOP BB9 (*n* = 17)	0.00008	0.000005	0.281676	0.000013	1.46726	1.88687	−26.8	0.4
UFOP BB10 (*n* = 13)	0.00016	0.000010	0.281677	0.000014	1.46725	1.88669	−26.8	0.5
UFOP BB11 (*n* = 12)	0.00010	0.000006	0.281676	0.000008	1.46726	1.88679	−26.8	0.3
UFOP BB12 (*n* = 15)	0.00015	0.000009	0.281677	0.000011	1.46725	1.88679	−26.8	0.4
UFOP BB13 (*n* = 12)	0.00004	0.000003	0.281675	0.000009	1.46726	1.88680	−26.8	0.3
UFOP BB14 (*n* = 9)	0.00005	0.000003	0.281678	0.000010	1.46727	1.88670	−26.7	0.4
UFOP BB16 (*n* = 16)	0.00005	0.000003	0.281676	0.000009	1.46726	1.88679	−26.8	0.3
UFOP BB17 (*n* = 11)	0.00005	0.000003	0.281677	0.000006	1.46725	1.88680	−26.8	0.2
UFOP BB18 (*n* = 16)	0.00012	0.000007	0.281675	0.000010	1.46725	1.88678	−26.9	0.4
UFOP BB ALL	0.00009	0.000005	0.281676	0.000010	1.46726	1.88678	−26.8	0.4

JWG, J.W. Goethe University of Frankfurt am Main; UFOP, Federal University of Ouro Preto. εHf561 calculated as an initial value for the age 561 Ma obtained by U-Pb dating of BB zircon. Individual analyses are reported in online supporting information.

Oxygen isotopic systematics

Our SIMS results are reported in Table 9, and a photo of the sample mount can also be downloaded from the electronic appendix(Appendix B).Twenty-seven interspersed analyses of the 91500 zircon determined from a single mm-sized area showed no significant drift in the observed $^{18}O^{-}/^{16}O^{-}$ over the course of the 17 hour run. Hence no drift correction was necessary. Another group of n = 30 determinations on a total of three chips from 91500 yielded a value for the total fractionation of 1.0022268 ± 0.24 ‰ (2SD); this value being based on the assigned $\delta^{18}O$ SMOW composition for 91500 of 9.98 ‰ (Wiedenbeck *et al*. 2004). This value for instrumental bias was applied to all other oxygen isotope ratio results obtained during this study. The three quality control materials Penglai (Li *et al*. 2010), Plešovice and Temora2 (Black *et al*. 2004) all gave results that were within 0.4 ‰ of their published values, so we conclude that our data are reliable with an overall uncertainty of better than ± 1 ‰ (2SD). The source of the systematic offset between 91500 and the other reference materials remains unclear and this pattern has been seen in other, as yet unpublished, data sets from the Potsdam lab. We suspect this effect might be related to the lack of a well-established traceability chain between the assigned values for the various materials.

The four BB zircon crystals studied during the oxygen part of this project all produced similar $\delta^{18}O$ SMOW values, with an overall mean of 13.16 ± 0.78 ‰ (n = 109, 2SD); this result is similar to the value of $\delta^{18}O$ = 13.9 for the M257 Sri Lankan gem reference material reported by Nasdala *et al*. (2008), but contrast with the value of $\delta^{18}O$ = 8.3 reported for M127 reference materials (Nasdala *et al*.2016), which is also of Sri Lankan origin (Figure 12). The overall $\delta^{18}O$ reproducibility on the four BB samples of only ± 0.78 ‰ (2SD) indicates that real oxygen isotope ratio variations exists within the BB sample suite. A closer look reveals that the BB9 and BB12 crystals are some 0.5 ‰ heavier in their oxygen isotope compositions than is the case for the BB25 and BB39 crystals. Of the four grains which were studied for oxygen isotope

systematics, the BB39 crystal shows the best reproducibility at ± 0.20 ‰ (2SD, n= 30 determinations on n = 3 fragments, 2SD). This is as good as the reproducibility determined for both the 91500 primary calibrant as well as the Penglai and Plešovice quality control materials, and hence we conclude from our data set there is no evidence for oxygen isotope heterogeneity in the BB39 crystal. The other three crystals show significantly larger values for their reproducibility, which we interpret as showing real natural heterogeneity. The overall range for the entire suite of BB material investigated here is small (± 0.78 ‰ - 2SD), suggesting that the material may be cogenetic in its origin.

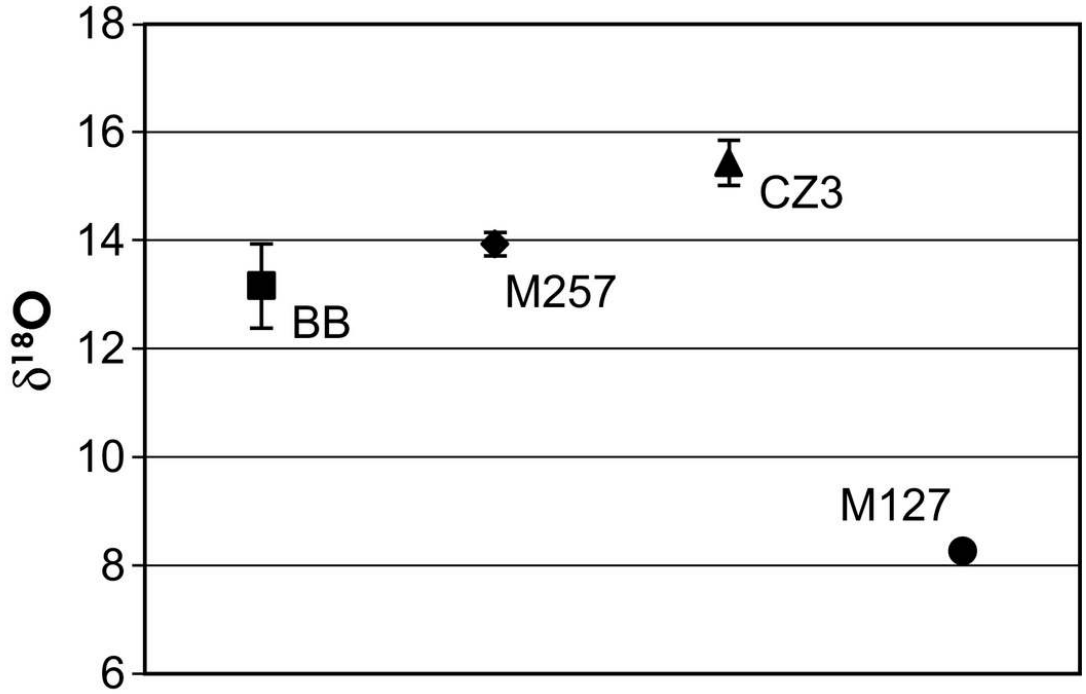

Figure 12: $\delta^{18}O$ SMOW values of BB, M257, CZ3 and M127 zircons

Table 9: Summary of results from SIMS oxygen isotope investigation

Reference material	Number of fragments/grains analysed	Number of analyses	$\delta^{18}O$ SMOW (per mil, 1*s*)	Repeatability (per mil, 2*s*)	Published value for RM (2*s* uncert.)
91500	3	30	9.86[a]	0.24	9.86 ± 0.22 Wiedenbeck *et al.* (2004)
Penglai	2	20	4.91	0.26	5.31 ± 0.10 Li *et al.* (2010)
Plešovice	2	19	7.9	0.22	8.19 J.W. Valley (unpublished data)
Temora 2	14	21	7.97	0.34	8.2 Black *et al.* (2004)
BB9	3	31	13.5	0.56	This study
BB12	3	29	13.43	0.32	
BB25	2	19	12.74	0.34	
BB39	3	30	12.83	0.20	

All values reported in this table are simple means of the stated number of analytical results. a Zircon 91500 was used as the calibration material for determining the absolute δ18O values of all other materials. Hence, its result is the assigned literature value.

Comparison with other Sri Lankan reference zircons and comments on origin

The relatively consistent chemical and physical properties, including their outstanding megacrystic size (several mms),of Sri Lankan zircons from the Ratnapura district underlies the reasoning for their use as international intra-laboratory reference material, specifically samples SL7 (Kinny *et al.* 1991), CZ3 (Pidgeon *etal.* 1994), M257 (Nasdala *et al.* 2008) and BR266 (Stern 2001) are in common use for Pb-U and/or Lu-Hf-isotope analyses, especially for ion probe analyses. For laser ablation ICP-MS analysis, Gehrels *et al.*(2008)used a Sri Lankan zircon crystal as a primary age calibration material.

Ratnapura zircons, as a group, have high $\delta^{18}O$ values, values much greater than mantle values (~5.1‰,Valley 2003) and all above ~ 13 ‰ VSMOW (Vienna Standard Mean Ocean Water). This isotopic feature indicates a significant surficial component was incorporated in the

source rocks at the depth of crystallization either in a metamorphic or igneous setting. Cathodoluminescence patterns are variable, from oscillatory zoning typically assigned to igneous types (Chakoumakos *et al.* 1987, Kröner *et al.* 1987)to broad, bland zoning ascribed to high grade metamorphic zircons. Based on the high oxygen isotope ratios, Cavosie *et al.* (2011) proposed that these Ratnapura megacrysts must have a metamorphic origin, probably a marble or Ca-silicate skarn. Determining the petrogenesis for BB zircons was not a specific goal of this paper, but a metamorphic origin appears likely.

The SL7, CZ3, M257, BR266 and the Sri Lankan reference materials of Gehrels *et al.*(2008) and the BB zircons have average U contents of 2678 μg g^{-1}, 551 μg g^{-1}, 840 μg g^{-1}, 909 μg g^{-1}, 518 μg g^{-1} and a variation ranges from 227 to 368 μg g^{-1}, Th/U ratios of 0.15 (Kinny *et al.* 1991), 0.06 (Pidgeon *et al.* 1994), 0.27 (Nasdala *et al.* 2008), 0.22 (Stern 2001), 0.13 (Gehrels *et al.*2008) and averages between 0.20 and 0.47 (for different grains; this study), respectively. In addition, the SL7, BR266 and M257 show only small variations in their REE mass fraction as compared to our data from the BB zircons; however all of these materials show the same general REE pattern (steep chondrite-normalized patterns enriched in HREE relative to LREE, small negative Eu and positive Ce anomalies).This pattern is very different from patterns of a number of igneous zircons, such as M127 zircon (Figure 12), and support the interpretation of Cavosie *et al.*(2011), that the Ratnapura zirconsare derived from a marble or Ca-silicate skarn. It is notable that all of the measured Th/U, except CZ3, are significantly higher than 0.1, probably suggesting that the source of the zircons are not pelitic.

Furthermore, these Sri Lankan zircon reference materials have very similar $^{206}Pb/^{238}U$ ages and $^{176}Hf/^{177}Hf$ values (Table 10), also implying a common metamorphic history. The initial$^{176}Hf/^{177}Hf$ of the SL7, CZ3 and BB zircon corresponds to aε_{Hf} of approximately -23.0 (Kinny *et al.* 1991), -25.5 (Xu *et al.* 2004) and -26.8 (this work), respectively, suggestive of a substantial crustal history.

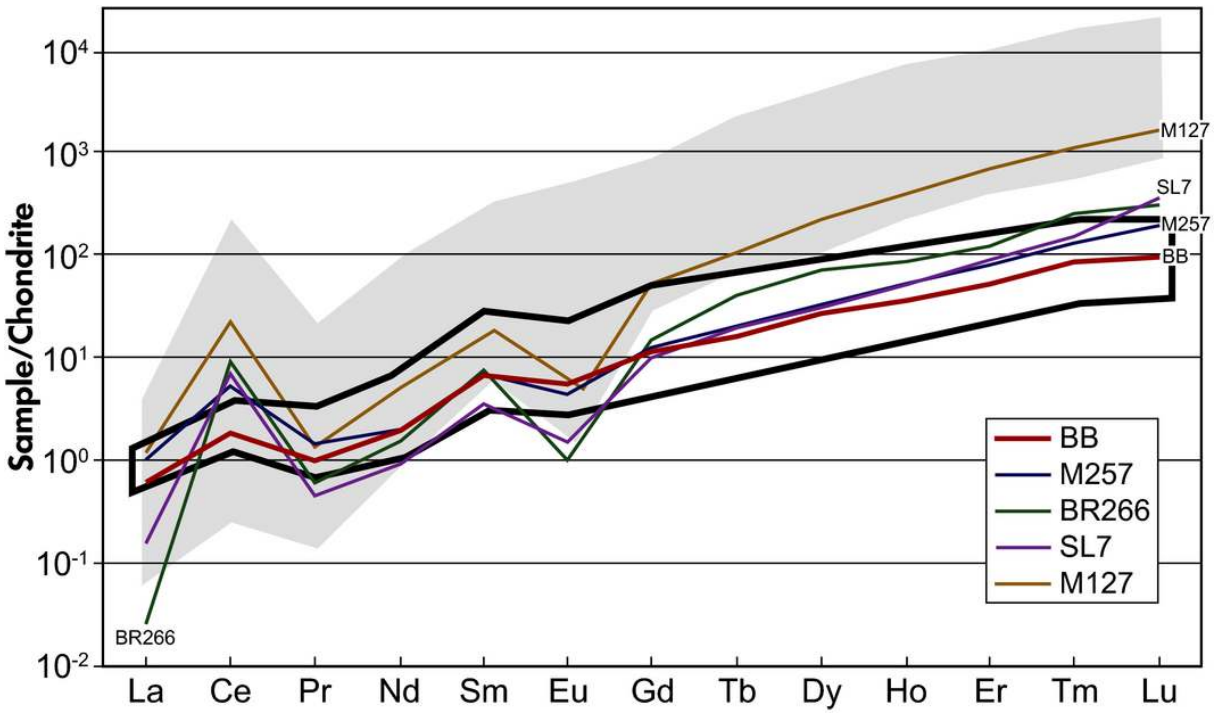

Figure 13: Chondrite-normalised grain rare earth element (REE) (average) composition of the BB, M257, BR266, SL7 and M127 zircons. The black line delimits the field for several analyses of BB zircons and the grey area indicates REE mass fraction ranges obtained for igneous zircon (graphically extracted from figure 2 in Hoskin and Schaltegger [**2**] and figure 2 in Nasdala *et al*. [**3**]).

Table 10: Summary of U-Pb age and Hf data for Sri Lankan zircons

Reference material	Age (± 1*s*, Ma)	$^{176}Hf/^{177}Hf$ (± 2*s*)	Reference
SL7	569 ± 3	0.28160 ± 0.00006[b]	Kinny *et al.* (1991)
CZ3	564 ± 2	0.281704 ± 0.000017[c]	Pidgeon *et al.* (1994), Xu *et al.* (2004)
BR266	559 ± 0.3	0.281624 ± 0.000024[c]	Stern (2001), Woodhead *et al.* (2004)
M257	561 ± 0.3	0.281544 ± 0.000018[c]	Nasdala *et al.* (2008), Hu *et al.* (2012)
Sri Lanka	564 ± 2		Gehrels *et al.* (2008)
BB9	561 ± 2[a]	0.281674 ± 0.000018[c]	This study

[a] $^{206}Pb/^{238}U$ ID-TIMS age of BB9 zircon; [b] TIMS Hf isotope analyses; [c] LA-MC-ICP-MS Hf.

Conclusions

The BB zircon crystals constitute a suitable reference material for LA-ICP-MS analysis of zircon. Based on a number of high quality techniques, including ID-TIMS and LA-ICP-MS, we were able to demonstrate that the BB zirconis a suitable normalization and quality control reference material for both U-Pb and Lu-Hf isotopic systems, provided that analyses target pristine CL-dark grain domains. The homogenous domains make up the majority of the crystals and can be easily separated from zones of fracture-controlled alteration and recrystallization. Various crystals were tested in a number of LA-ICP-MS analytical set-ups and were shown to be concordant to somewhat normally discordant. Individual fragments of the BB zircons have minor U-Pb age variation (0.4% RSD) that is only detectable by ID-TIMS analysis and is within uncertainty of the age precision obtained with LA-ICP-MS (*ca*. 1-2%,2SD). The BB crystals are marked by very low levels of initial common Pb and high uranium and radiogenic lead mass fractions, yielding high count rates and good counting statistics. The LA-ICP-MS data from six different LA-ICP-MS laboratories (n = 635points) gave mean ages of 564 ± 33 Ma (2SD, $^{207}Pb/^{206}Pb$), 562 ± 9 Ma (2SD, $^{206}Pb/^{238}U$) and 562 ±

10 Ma (2SD, $^{207}Pb/^{235}U$). Using BB9 zircon as a reference material, and assuming mean TIMS ages reported in Table 6b, yields concordia ages for a range of zircon reference materials within uncertainty of their published ages. We therefore conclude that the BB crystals perform well as either primary calibration or as a quality control materials for LA-ICP-MS U-Pb geochronology, and that the BB sample suite will be a useful addition to other materials available.

Laser ablation MC-ICP-MS analyses yielded low Lu/Hf (average of 0.00008) and Yb/Hf (average of 0.000005) ratios, which simplifies the task of isobaric interference correction, resulting in a better analytical uncertainty for the corrected $^{176}Hf/^{177}Hf$ ratios. The mean $^{176}Hf/^{177}Hf$ value of 0.281674 ± 0.000018(2SD) is considered the best estimate of the Hf isotopic composition of the BB zircon and is valid for any random chip to be used as a reference sample.

Cathodoluminescence imaging shows a remarkably high degree of internal homogeneity for large parts of individual crystals. The same applies to some trace element mass fractions, as variations in chemical composition, determined by LA-ICP-MS analyses, did not exceed experimental uncertainties. Some fractured and re-sealed, CL-bright domains are, however, clearly depleted in some trace and REE elements and yield ca. 10 m.y. younger U-Pb ages. Further analysis will be required to demonstrate that BB zircon can be used as a reference material for in-situ REE analyses.

Finally, our SIMS results on the oxygen isotope ratio of the BB zircons have shown that the inter-grain variations are fairly modest and the oxygen isotope heterogeneity with some of the single samples is small enough that these might in the future prove to be useful calibrants for $\delta^{18}O$ determinations by SIMS.

Acknowledgements

This work was funded by CNPq (projects 402852/2012-5, 401334/2012-0, 302633/2011-1, 305284/2015-0), FAPEMIG (projects CRA RDP00067-10, APQ03943 and APQ-01448-15), FINEP (project CT-INFRA) and PROPP/UFOP (03/2014 and 02/2015). We would like to acknowledge help from Adriana Tropia, José Cirilo Pereira and Antônio Celso Torres for assistance with lab preparation. Maristella Santos acknowledges scholarship from CAPES. ISB acknowledges support from the National Research Foundation (South Africa) and the CNPq (Science without Borders Program, Brazil). U. Dittmann and F. Couffignal played key roles in sample preparation and the subsequent analysis of the BB material for oxygen isotope systematics. We thank L. Nasdala and J. Sláma for providing reference materials M127 and Plešovice respectively.

References

Batumike J.M., Griffin W.L., Belousova E.A., Pearson N.J., O'Reilly S.Y., and Shee S.R. (2008)
LAM-ICPMS U–Pb dating of kimberlitic perovskite: Eocene–Oligocene kimberlites from the Kundelungu Plateau, D.R. Congo. **Earth and Planetary Science Letters, 267,** 609-619.

Black L.P., Kamo S.L., Allen C.M., Aleinikoff J.N., Davis D.W., Korsch R.J. and Foudoulis C. (2003)
TEMORA 1: a new zircon standard for phanerozoic U‑Pb geochronology. **Chemical Geology, 200,** 155-170.

Black L.P., Kamo S.L., Allen C.M., Davis D.W., Aleinikoff J.N., Valley J.W., Mundil R., Campbell I.H., Korsch R.J., Williams I.S. and Foudoulis C.(2004)
Improved Pb-206/U-218microprobe geochronology by the monitoring of a trace-element related matrix effect; SHRIMP, ID-TIMS, ELA-ICP-MS and oxygen isotope documentation for a series of zircon standards. **Chemical Geology, 205,** 115-140.

Cavosie A.J., Valley J.W., Kita N.T., Spicuzza M.J., Ushikubo T. and Wilde S.A.(2011)
The origin of high $\delta^{18}O$ zircons: marbles, megacrysts, and metamorphism. **Contributions to Mineralogy and Petrology, 162,** 961-974.

Chakoumakos B.C., Murakami T., Lumpkin G.R. and Ewing R.C.(1987)
Alpha-decay induced fracturing in zircon – the transition from the crystalline to the metamict state. **Science, 236,** 1556–1559.

Cherniak D.J. and Watson E.B. (2001)
Pb diffusion in zircon. **Chemical Geology, 172,** 5-24.

Cherniak D. J. and Watson B.(2003)
Diffusion in zircon. **In: Hanchar J.M. and Hoskin P.W.O. (eds), Zircon. Reviews in Mineralogy and Geochemistry, 53,**113-143.

Crowley J.L., Schoene B. and Bowring S.A. (2007)
U-Pb dating of zircon in the Bishop Tuff at the millennial scale. **Geology, 35,** 1123-1126.

Dewaele S., Henjes-Kunst F., Melcher F., Sitnikova M., Burgess R., Gerdes A., Fernandez M.A., Clercq F., Muchez P. and Lehmann B.(2011)
Late Neoproterozoic overprinting of the cassiterite and columbite-tantalite bearing pegmatites of the Gatumba area, Rwanda (Central Africa). **Journal of African Earth Sciences, 61,** 10-26.

Dharmapriya P.L., Malaviarachchi S.P.K., Santosh M., Tang L. andSajeev K. (2015)
Late-Neoproterozoic ultrahigh-temperature metamorphism in the Highland Complex, Sri Lanka. **Precambrian Research,271,** 311-333.

Dissanayake, C.B. and Rupasinghe, M.S. (1993)
A prospector's guide map of the gem deposits of Sri Lanka. **Gems and Gemology, 29,** 173-181.

Dissanayake C.B., Chandrajith R. and Tobschall H.J. (2000)
The geology, mineralogy and rare element geochemistry of the gem deposits of Sri Lanka. **Bulletin of the Geological Society of Finland, 72,** 5-20.

Gehrels G.E., Valencia V. and Ruiz, J.(2008)
Enhanced precision, accuracy, efficiency, and spatial resolution of U-Pb ages by laser ablation–multicollector–inductively coupled plasma–mass spectrometry. **Geochemistry, Geophysics, Geosystems, 9,**Q03017, doi:10.1029/2007GC001805.

Gonçalves G.O., Lana C, Scholz R,, Buick I.S., Gerdes A., Kamo S.L., Corfu F., Marinho M.M., Chaves A.O., Valeriano C. and Nalini Jr H.A.(2016)
An assessment of monazite from the Itambé pegmatite district for use as U–Pb isotope reference material for microanalysis and implications for the origin of the "Moacyr" monazite. **Chemical Geology, 424,** 30-50.

Griffin W.L., Pearson N.J., Belousova E.A. andSaeed A. (2006)
Comment: Hf-isotope heterogeneity in zircon 91500. **Chemical Geology, 233,** 358-363.

Gulson B.L. and Jones M.T. (1992)
Cassiterite: Potential for direct dating of mineral deposits anda precise age for the Bushveld Complex granites. **Geology, 20,** 355-358.

Hölzl S., Hofmann A.W., Todt W. and Kiihler H. (1994)
U-Pb geochronology of the Sri Lankan basement. **Precambrian Research, 66,** 123-149.

Hoskin P.W.O. and Schaltegger U. (2003)
The composition of zircon and igneous and metamorphic petrogenesis. In: Hanchar J.M. and Hoskin P.W.O. (eds), Zircon. Reviews in Mineralogy and Geochemistry, 53,27–62.

Hu Z., Liu Y., Gao S., Liu W., Zhang W., Tong X., Lin L., Zong K., Li M., Chen H., Zhou L. and Yang L. (2012)
Improved in situ Hf isotope ratio analysis of zircon using newly designed X skimmer cone and jet sample cone in combination with the addition of nitrogen by laser ablation multiple collector ICP-MS. **Journal of Analytical Atomic Spectrometry, 27,** 1391-1399.

Jackson S.E., Pearson N.J., Griffin W.L. and Belousova E.A. (2004)
The application of laser ablation-inductively coupled plasma-mass spectrometry to in situ U–Pb zircon geochronology. **Chemical Geology,211,** 47-69.

Jaffey A.H., Flynn K.F., Glendenin L.E., Bentley W.C., Essling A.M. (1971)
Precision measurement of half-lives and specific activities of ^{235}U and ^{228}U.**Physical Review C 4,** 1889-1906.

Kinny P.D., Compston W. and Williams I.S. (1991)
A reconnaissance ion-probe study of hafnium isotopes in zircons. **Geochimica et Cosmochimica Acta, 55,** 849-859.

Kröner A., Jaeckel P. and Williams I.S.(1994a)
Pb-loss patterns in zircons from a high-grade metamorphic terrain as revealed by different dating methods: U–Pb and Pb–Pb ages for igneous and metamorphic zircons from northern Sri Lanka. **Precambrian Research, 66,** 151-181.

Kröner A., Kehelpannala K.V.W. and Kriegsman L.M. (1994b)
Origin of compositional layering and mechanism of crustal thickening in the high-grade gneiss terrain of Sri Lanka. **Precambrian Research, 66,** 21-37.

Kröner A., Williams I.S., Compston W., Baur N., Vitanage P.W. andPerera R.K.(1987)
Zircon ion-microprobe dating of high-grade rocks in Sri Lanka. **The Journal of Geology, 95,** 775-791.

Li X.H., Long W.G., Li Q.L., Liu Y., Zheng Y.F.,Yang Y.H., Chamberlain K.R., Wan D.F., Guo C.H.,Wang X.C. andTaoH.(2010)
Penglai zircon megacrysts: A potential new working reference material for microbeam determination of Hf-O isotopes and U-Pb age. **Geostandards and Geoanalytical Research, 34,** 117-134.

Mattinson J.M. (2010)
Analysis of the relative decay constants of ^{235}U and ^{238}U by multi-step CA-TIMS measurements of closed-system natural zircon samples. **Chemical Geology, 275,**186-198.

Morel M.L.A., Nebel O., Nebel-Jacobsen Y.J., Miller J.S. and Vroon P.Z. (2008)
Hafnium isotope characterization of the GJ-1 zircon reference material by solution and laser-ablation MC-ICPMS. **Chemical Geology, 255,** 231-235.

Murakami T., Chakoumakos B.C., Ewing R.C., Lumpkin G.R. andWeber W.J.(1991)
Alpha-decay event damage in zircon. **American Mineralogist, 76,** 1510-1532.

Nasdala L., Irmer G. andWolf D. (1995)
The degree of metamictization in zircon: a Raman spectroscopic study. **European Journal of Mineralogy, 7,** 471-478.

Nasdala L., Wenzel M., Vavra G., Irmer G., Wenzel T. and Kober B. (2001)
Metamictisation of natural zircon: accumulation versus thermal annealing of radioactivity-induced damage. **Contributions to Mineralogy and Petrology, 141,** 125-144.

Nasdala L., Reiners P.W., Garver J.I., Kennedy A.K., Stern R.A., Balan E. and Wirth R. (2004)
Incomplete retention of radiation damage in zircon from Sri Lanka. **American Mineralogist, 89,** 219-231.

Nasdala L., Hofmeister W., Norberg N., Martinson J.M., Corfu F., Dörr W., Kamo S.L., Kennedy A.K., Kronz A., Reiners P.W., Frei D., KošlerJ., Wan Y., Götze J., Häger T., Kröner A. and Valley J.W. (2008)
Zircon M257 - a homogeneous natural reference material for the ion microprobe U-Pb analysis of zircon. **Geostandards and Geoanalytical Research, 32,** 247-265.

Nasdala L., Corfu F., Valley J.W., Spicuzza M.J., Wu F., Li Q., Yang Y., Fisher C., Münker C., Kennedy A.K., Reiners P.W., Kronz A., Wiedenbeck M., Wirth R., Chanmuang C., Zeug M., Váczi T., Norberg N., Häger T., Kröner A. and Hofmeister W. (2016)
Zircon M127 – A homogeneous reference material for SIMS U-Pb geochronology combined with hafnium, oxygen and, potentially, lithium isotope analysis. **Geostandards and Geoanalytical Research,** doi: 10.1111/ggr.12123.

Pidgeon R.T., Furfaro D., Kennedy A.K., Nemchin A.A. and Van Bronswijk W. (1994)
Calibration of zircon standards for the Curtin SHRIMP II. **In: Eighth International Conference on Geochronology, Cosmochronology, and Isotope Geology - Abstracts: United States Geological Survey Circular, 1107,** 251.

Sajeev K., Williams I.S. and Osanai Y. (2010)
Sensitive high-resolution ion microprobe U-Pb dating of prograde and retrograde ultrahigh-temperature metamorphism as exemplified by Sri Lankan granulites.**Geology, 11,** 971-974.

Santosh M., Tsunogae T., Malaviarachchi S.P.K., Zhang Z.M., Ding H.X., Tang L. and Dharmapriya P.L.(2014)
Neoproterozoic crustal evolution in Sri Lanka: insightsfrom petrologic, geochemical and zircon U–Pb and Lu–Hf isotopic data andimplications for Gondwana assembly. **Precambrian Research, 255,** 1-29.

SchmitzM.D. and Schoene B.(2007)
Derivation of isotope ratios, errors and error correlations for U–Pb geochronology using ^{205}Pb–^{235}U–(^{233}U)-spiked isotope dilution thermal ionization mass spectrometric data. **Geochemistry, Geophysics, Geosystems,8,**Q08006, doi:10.1029/2006GC001492.

Schoene B., Crowley J.L., Condon D. J., Schmitz M.D. and Bowring S.A. (2006)
Reassessing the uranium decay constants for geochronology using ID-TIMS U–Pb data. **Geochimica et Cosmochimica Acta, 70,** 426-445.

Sláma J., Košler J., Condon D.J., Crowley J.L., Gerdes A., Hanchar J.M., Horstwood M.S.A., Morris G.A., Nasdala L., Norberg N., Schaltegger U., Schoene B., Tubrett M.N. and Whitehouse M.J.(2008)
Plešovice zircon – a new natural reference material for U–Pb and Hf isotopic microanalysis. **Chemical Geology, 249,** 1-35.

Speer J.A.(1982)
Zircon. **In: Ribbe P.H. (Ed.), Orthosilicates. Mineralogical Society of America Reviews in Mineralogy, 5,**67-l12.

Stern R.A.(2001)
A new isotopic and trace element standard for the ion microprobe: preliminary TIMS U–Pb and electron microprobe data, current research. **Radiogenic Age and Isotopic Studies: Report 14. Geological Survey of Canada**, Ottawa, Canada 120p.

Taylor S.R. and McLennan S.M.(1985)
The Continental Crust: its Composition and Evolution. **Blackwell, Oxford,** 312 pp.

Valley J.W.(2003)
Oxygen isotopes in zircon. **In: Hanchar J.M. and Hoskin P.W.O. (eds), Zircon. Reviews in Mineralogy and Geochemistry, 53,** 343-380.

Valley J.W., Lackey J.S., Cavosie A.J., Clechenko C.C., Spicuzza M.J., Basei M.A.S., Bindeman I.N., Ferreira V.P., Sial A.N., King E.M., Peck W.H., Sinha A.K. and Wei C.S.(2005)
4.4 billion years of crustal maturation: oxygen isotope ratios of magmatic zircon. **Contributions to Mineralogy and Petrology, 150,**561-580.

Wiedenbeck M., Allé P., Corfu F., Griffin W.L., Meier M., Oberli F., von Quadt A., Roddick J.C. and Spiegel W.(1995)
Three natural zircon standards for U-Th-Pb, Lu-Hf, trace element and REE analyses. **Geostandards Newsletter, 19,** 1-23.

Wiedenbeck M., Hanchar J.M., Peck W.H., Sylvester P., Valley J.W., Whitehouse M.J., Kronz A., Morishita Y., Nasdala L., Fiebig J., Franchi I., Girard J.P., Greenwood R.C., Hinton R., Kita N., Mason P.R.D., Norman M., Ogasawara M., Piccoli R., Rhede D., Satoh H., Schulz-Dobrick B., Skar O., Spicuzza M.J., Terada K., Tindle A., Togashi S., Vennemann T., Xie Q. and Zheng Y.F. (2004)
Further characterisation of the 91500 zircon crystal. **Geostandards and Geoanalytical Research, 28,** 9-39.

Woodhead J.D. and Hergt J.M. (2005)
Preliminary appraisal of seven natural zircon reference materials for in situ Hf isotope determination. **Geostandards and Geoanalytical Research, 29,** 183-195.

Woodhead J.D., Hergt J.M., Shelley M., Eggins S. and Kemp R. (2004)
Zircon Hf-isotope analysis with an excimer laser, depth profiling, ablation of complex geometries and concomitant age estimation. **Chemical Geology, 209,** 121-135.

Xu P., WuF.Y., Xie L.W. and Yang Y.H. (2004)
Hf isotopic compositions of the standard zircons for U–Pb dating. **Chinese Science Bulletin, 49,** 1642-1648.

ZhiChao L., Yuan W. F., ChunLi G., ZiFu Z., JinHui Y. and JinFeng S.(2011)
In situ U-Pb dating of xenotime by laser ablation (LA)-ICP-MS. **Chinese Science Bulletin, 56,** 2948-2956.